Spring 2011

A Pilot Model for Investigating Biodynamic Coupling Due to Aeroservoelastic Accelerations

Brandon Cowen
Old Dominion University

A PILOT MODEL FOR INVESTIGATING BIODYNAMIC COUPLING DUE TO

AEROSERVOELASTIC ACCELERATIONS

by

Brandon Cowen
B S December 2007, Embry Riddle Aeronautical University

A Thesis Submitted to the Faculty of
Old Dominion University in Partial Fulfillment of the
Requirements for the Degree of

MASTER OF SCIENCE

AEROSPACE ENGINEERING

OLD DOMINION UNIVERSITY
May 2011

Approved by

_____
Thomas Alberts (Director)

_____
Jeremiah Creedon (Member)

_____
Brett Newman (Member)

_____
Keith Hoffler (Member)

ABSTRACT

A PILOT MODEL FOR INVESTIGATING BIODYNAMIC COUPLING DUE TO AEROSERVOELASTIC ACCELERATIONS

Brandon Cowen
Old Dominion University, 2011
Dr Thomas Alberts

Supersonic Transport Aircraft tend to have slender fuselages with respect to their subsonic counterparts This design feature leads to increased aeroservoelastic bending at low resonant frequencies closer to the frequencies of pilot commands and the corresponding rigid body accelerations Aeroelastic accelerations of certain frequencies and phase lags at the pilot station have been seen to involuntarily pass through the pilot's body to the control inceptor When the pilot commands rigid body accelerations in phase with the structural response, the structural accelerations grow Thus biodynamic coupling represents the coupling between the feedthrough of pilot station acceleration through the pilot's body, with the pilot control strategy A pilot model has been constructed to simulate the lateral-directional component of this interaction The model attempts to break down the biodynamic coupling phenomenon into involuntary biodynamic feedthrough and cognitive commands that include rigid body control strategy and the aeroservoelastic response The final model will generate maneuvers from predicted pilot control strategy and the resultant biodynamic feedthrough and coupling in the lateral axis when paired with an airplane model incorporating both rigid body and structural accelerations Utilizing the resulting model, the impact of the phase lag of each integral part of the total system will be studied and shown to drastically impact the overall level of biodynamic coupling

This thesis is dedicated to my parents

ACKNOWLEDGEMENTS

NOMENCLATURE

6DoF	Six Degree of Freedom
APC	Aircraft Pilot Coupling
ASE	Aeroservoelastic
BDC	Biodynamic Coupling
CMF	Cockpit Motion Facility
DASE	Dynamic Aeroservoelastic
FFT	Fast Fourier Transform
GA	Generic Airplane
HSCT	High-Speed Civil Transport
LaRC	Langley Research Center
LTI	Linear, Time-Invariant
NASA	National Aeronautics and Space Administration
NASTRAN	NASA Structural Analysis
P S	Pilot Station
Ref-H	Reference H (Cycle 4, Supersonic Transport Configuration)
SDSS	Supersonics Development and Simulation Study
VMS	Visual Motion Simulator

TABLE OF CONTENTS

LIST OF TABLES

LIST OF FIGURES

1. INTRODUCTION

Long, slender body aircraft such as supersonic transports experience increased dynamic aeroservoelastic accelerations at the pilot station This structurally exacerbated aeroelastic vibration feeds through a pilot's body involuntarily to the control inceptor and thus to the flight control system The relative phase of this feedthrough to the pilot control inputs will determine if the structural accelerations grow This phenomenon is known as biodynamic coupling Biodynamic coupling represents a closed-loop system, where the individual contribution of each component of the total pilot-aircraft system influences the response of the entire system Thus, to further understand this phenomenon and analyze the effects of phase lags of each component of the pilot-airplane system, a pilot model of the system has been developed This pilot model will be composed of two main components, a crossover model for prediction of pilot control strategy, and a model for prediction of the physical, involuntary feedthrough

The nature of the pilot control strategy directly impacts the resulting amount of biodynamic coupling Pilot control inputs lead to structural accelerations and thus pilot station accelerations when enough rigid body motion near the dominant structural resonant mode frequency is commanded This acceleration can grow or diverge given pilot inputs of the right frequency and phase with respect to the structural accelerations Pilot control strategy can also have the opposite effect Pilots and human operators generally adapt their control strategy depending on the nature of the controlled plant and primary task (1) However, the primary task of the pilot generally is to maneuver the aircraft to certain desired states This thesis will describe a model of pilot control strategy for a generic lateral offset landing task, where the primary task of the pilot is to safely land the aircraft while targeting desired landing performance metrics As a result of the difficulty of the landing task, it is assumed that the pilot is unable to adapt his/her pilot control strategy strictly due to the influence of pilot station accelerations after an initial learning period

A pilot model intended to predict pilot control strategy was derived based on several piloted simulation studies performed at NASA Langley Research Center (LaRC) The resulting model simulates a typical, noisy, pilot control response, based on results from a piloted study involving a lateral offset landing maneuver The model structure is based on a simplified form of the Hess multi-loop structural model to predict control strategy, using approximations for neuromuscular lag, and visual and vestibular systems from conventional pilot modeling theory (2)

Biodynamic coupling depends directly on the level of physical, involuntary feedthrough of pilot station accelerations through the pilot torso and arm to the stick Similar to pilot control inputs, involuntary feedthrough can cause the structural accelerations to grow providing that the resulting involuntary pilot commands are of the right frequency and phase with respect to the structural accelerations are present

The pilot model predicts levels of involuntary biodynamic feedthrough based on results from a piloted study where pilots were subjected to accelerations over a range of frequencies and amplitudes The resulting stick deflections were then recorded as a primary dependent variable of the system, and along with the known motion base accelerations, used to model the direct relationship between pilot station acceleration and physiological feedthrough into the stick

The ability of the pilot model to simulate both an intentional pilot control response and involuntary biodynamic feedthrough allows for complete analysis of the biodynamic coupling phenomenon By looking at the phase relationship between the predicted pilot inputs, the structural response of the aircraft, and the corresponding involuntary biodynamic feedthrough, one can predict when biodynamic coupling will present itself, and which system characteristics are the main drivers

A complete model of the environment is needed to simulate the entire interaction between pilot and aircraft The following material will discuss how the pilot model, programmed in series with a 6 degree of freedom (6DoF) Generic Airplane model (GA)

with rigid and structural dynamics, generates a typical pilot command in the lateral axis based on a desired lateral offset position The command is then passed to the generic airplane model which translates that command into rigid body accelerations and then to aeroservoelastic accelerations at the pilot station The pilot station accelerations are then passed to the pilot model, closing the loop, with the expected feedthrough to the inceptor superimposed on the pilot's voluntary control strategy A high-level depiction of this system is shown in Figure 1 The modeled time delay of the motion base simulator will then be varied, to demonstrate how small changes in phase of a single component of the system will affect the overall level of biodynamic coupling experienced The time delay of the modeled motion base will be changed for this study, and removed completely to simulate actual flight These results will be compared to results predicted from piloted simulation studies and demonstrate the impact of motion base lag for studying biodynamic coupling
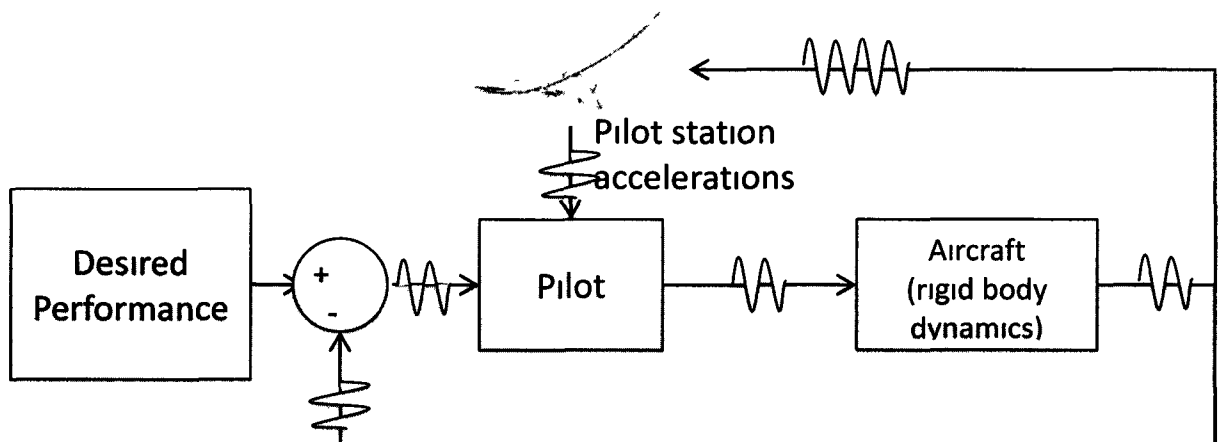
Figure 1 Biodynamic coupling

2. PAST AND CURRENT RESEARCH

2.1 Parametric Studies for Biodynamic Coupling

A piloted simulation study was performed at NASA LaRC's Visual Motion Simulator (VMS) in 1995 for a piloted assessment of the High-Speed Civil Transport Part of this study evaluated the impact of dynamic aeroservoelastic accelerations (DASE) on handling qualities of supersonic transports The HSCT is a full 6DoF rigid body and dynamic structural model to implement in a real-time simulation (3) The final version implemented during the piloted study was known as the Ref-H Cycle 4 configuration (4) This model included a full aircraft simulation with detailed models for control surfaces, engines, aerodynamic stability derivatives and industry-designed flight control systems A full DASE model was derived from a quasi-static aeroelastic model predicted from a full NASTRAN model of the HSCT (3)

The resulting piloted parametric study established that the accelerations at the pilot station resulting from the DASE model impacted handling qualities and caused biodynamic coupling (3) This issue was most severe during a landing task developed to generate a high urgency lateral offset maneuver Several solutions for preventing biodynamic coupling were explored, however, for an effective solution to be developed, more in depth knowledge of the problem is required

2.2 SDSS Project and Lateral Offset Task

The Supersonics Development and Simulation Study (SDSS) was initiated at NASA LaRC utilizing both the VMS and the newer and more capable Cockpit Motion Facility (CMF) in 2007 One of the technology items to be addressed is gaining understanding of the bio-dynamic coupling problem and studying potential solutions

The lateral offset task provided the main database of information for deriving the pilot model   This task was designed to force pilots to make large rapid lateral corrections near touchdown thus commanding rigid body motions large enough to excite the

structural models During the task the pilots are instructed to perform a benign 200 ft
lateral correction to the ILS starting at an altitude of 714 ft before commanding a larger
300 ft , and high urgency, lateral correction at 250 ft above sea level The pilots are in
the clouds until breakout at 250 ft , where they will have to make a left or right lateral
correction Figure 2 shows an illustration of the approach Figure 3 shows a picture of the
two different scenarios of what the pilots see after breaking out of the clouds, with a
left offset in the left picture and a right offset in the right The pilot is always
commanded to land on the runway on the right This maneuver would be not be
representative of a typical piloted task and represents a worst-case scenario

Figure 2 Lateral offset landing task – (3)

Figure 3 Breakout for lateral offset landing task

The aggressive landing performance metrics are shown in

Table 1 The task is designed to force the pilot to perform an aggressive lateral maneuver with defined metrics to keep the pilot tightly in the control loop This maximizes the potential for exciting the DASE and minimizes the amount of attention the pilots can appropriate towards adapting their control strategy specifically towards minimizing pilot station accelerations

Table 1 Lateral offset task performance metrics

Parameter	Target	Desired	Adequate
Airspeed deviation at 50 ft (kts)	0	+/- 5	+/- 10
Bank angle at 50 ft (°)	0	+/- 5	+/- 7
Lateral distance of c g from runway threshold (ft)	1250	+/- 250	-500, +1000
Longitudinal distance of c g from runway centerline (ft)	0	+/- 10	+/- 27
Vertical speed at touchdown (ft/s)	0	>= -4	>= -7
Landing heading error (°)	0	+/- 3	+/- 6

The SDSS task also added a lower urgency, localizer tracking and glideslope capture task before performing the final large lateral offset maneuver The pilots are required to capture and track a localizer from an initial offset of 200 ft and to capture a three degree glideslope shortly after the simulation run starts Performance metrics were not recorded for this portion of the task

Figure 4 and Figure 5 below demonstrate how quickly pilot station accelerations can feedthrough to pilot control inputs The first few seconds of Figure 4 illustrate the expected low frequency pilot inputs of a pilot tracking an initial 200 ft lateral offset As the structural model is excited around ten seconds, the presence of higher frequency content in the lateral stick deflection becomes apparent Figure 5 shows a pilot having particular difficulty in converging towards the desired lateral offset position, before the pilot reaches a breakout at 250 ft
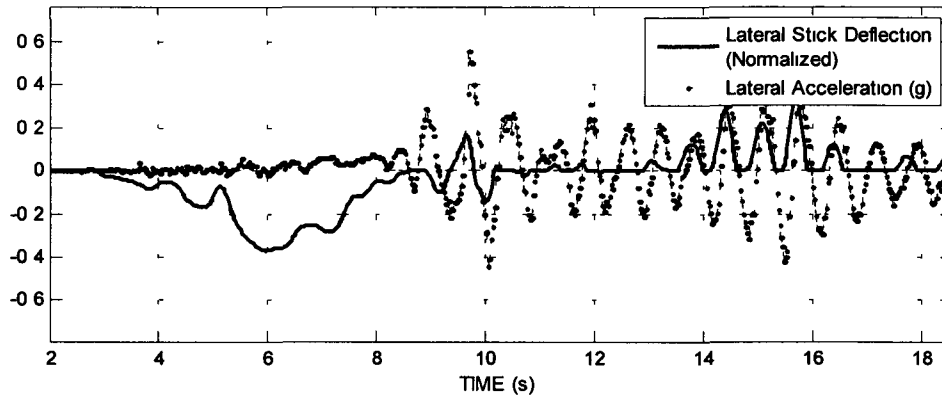
Figure 4 Time history of ILS tracking from run 812
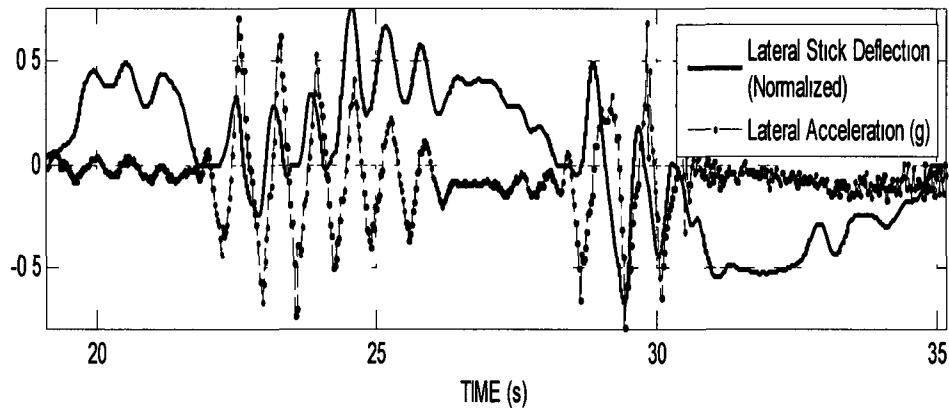
Figure 5 Intermediate segment (during ILS capture) of time history from Run 812

The resulting lateral stick deflection demonstrates the effects of the aeroelastic accelerations on the pilot's control inputs The aeroelastic accelerations due to the aircraft structure clearly feedthrough to the pilot inputs and degrade the pilot's ability to perform the lateral maneuver The feedthrough is evident in the alignment of the DASE motions and pilot inputs knowing that the pilot's inputs were not intentional Figure 5 illustrates how the frequency of the pilot's inputs converges towards the same frequency as the lateral acceleration as the lateral acceleration grows

As part of the research effort for the SDSS study, an analytical pilot model was developed in an attempt to completely model the pilot-airplane system The CMF motion characteristics were also modeled, to be presented in 3 The cognitive component of the pilot model, to be presented in later sections, predicts control strategy The bio-dynamic component of the pilot model includes a model for involuntary feedthrough to quantify the involuntary effects of the aeroelastic vibrations on the pilot In this initial attempt, the proposed model was designed to match pilot control strategy during the lateral offset maneuver from the SDSS study from runs performed without the presence of a DASE model Furthermore, the model is also limited to predicting lateral stick inputs, and modeling the physiological response from lateral accelerations only

Pilot control strategy and involuntary feedthrough combine to make the lateral-directional pilot model and represent a portion of the total pilot-airplane biodynamic coupling closed-loop system The following sections will present detailed models for the aircraft rigid body and structural dynamics and a model of the motion base simulator

3. SIMULATION AND FACILITIES DESCRIPTION

3.1 Generic Airplane

The Generic Airplane (GA) is a 6DoF aircraft dynamics model coded in Simulink The model is capable of representing a diverse range of aircraft at different levels of fidelity (5) The GA utilizes parabolic stick shaping passed to a pitch-rate command system in the longitudinal axis and a roll-rate command system in the lateral axis Commands are passed to first order lags representing the simulated roll mode time constant and short period mode, before being passed to first order servo-actuator lags which convert the input commands to moment commands The moment commands are then limited by specified maximum control surface authority and basic departure restraints based on normal acceleration and angle of attack limiters The resulting moments are then used to compute rigid body accelerations to compute the states at the next iteration based on the inertia and aerodynamic coefficients of the Ref-H Cycle 4 The GA uses simplified table look-ups for trimmed lift, drag, and side force coefficients and thrust, all based on Ref-H Cycle 4 data
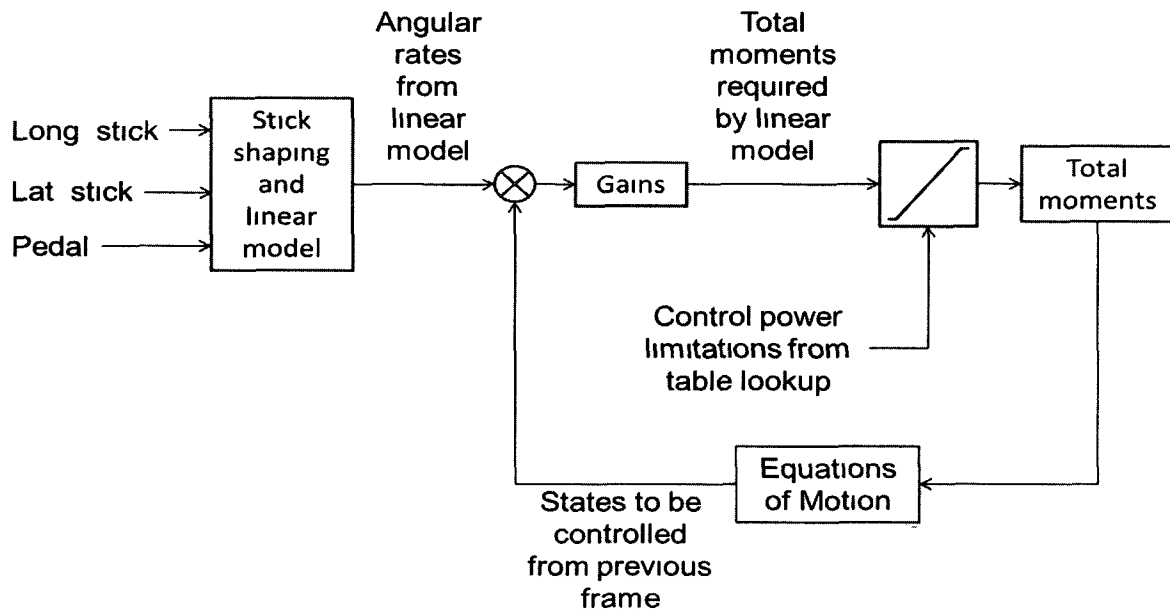
Figure 6 Generic Airplane

The GA contains a structural model that computes a deflection at the pilot station based on the required moment at the tail The resulting deflections represent an approximation derived from the HSCT Ref H Cycle 4 configuration These structural accelerations at the pilot station are superimposed over the rigid body accelerations The resulting pilot station deflections do not, however, feedback and thus influence the rigid body dynamics other than through the pilot The structural model is composed of a simple second order transfer function for each bending mode for both the symmetric (vertical) and anti-symmetric (lateral) axes The GA can represent up to the first three bending modes, however, for simplification of analysis, typically, only the first bending mode was modeled The second order transfer functions inherent in the model gave the capability of easily specifying various combinations of frequency and damping The range of frequencies and damping were derived from the Ref-H Cycle 4 model (6)
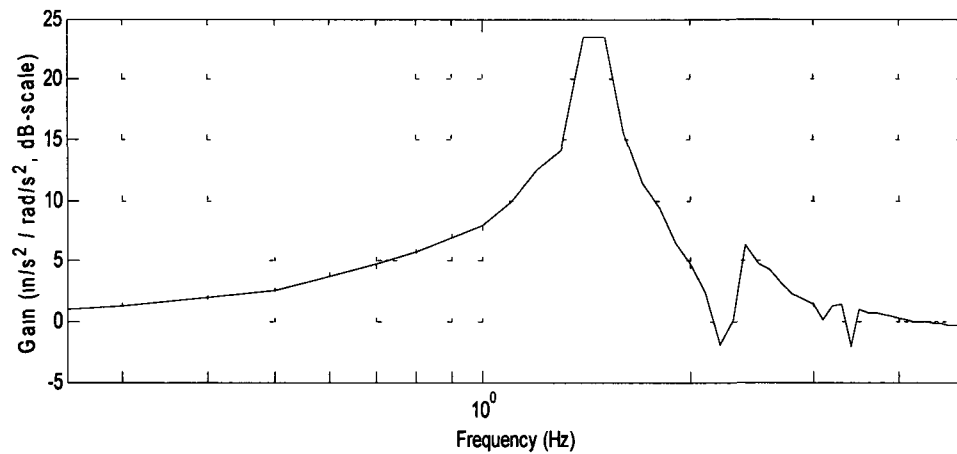
Figure 7   Symmetric and anti-symmetric amplitude ratio from rigid body to pilot station acceleration
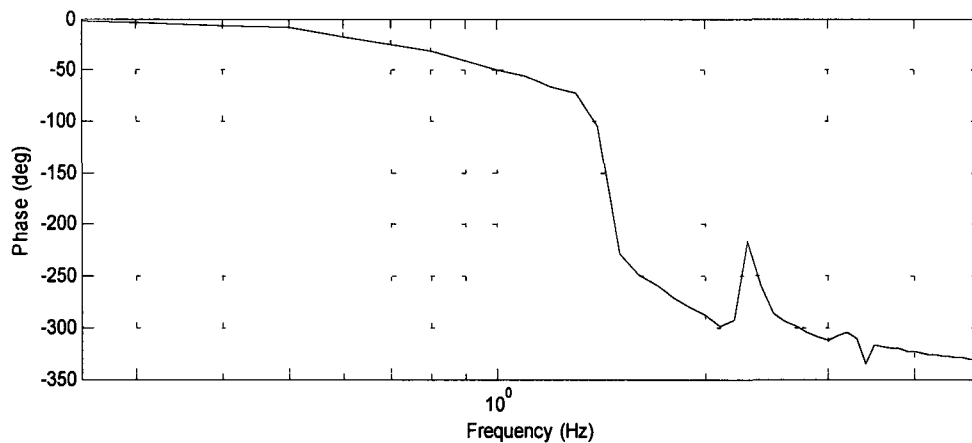
Figure 8   Symmetric and anti-symmetric phase lag from rigid body to pilot station acceleration

Figure 7 and Figure 8 show the corresponding lateral aeroservoelastic acceleration modeled at the pilot station resulting from rigid body angular acceleration (assumed from a given control surface force) at the aircraft centroid The cut off in peak in Figure 7 around 1 6 Hz is a result of the signal processing and a relatively coarse frequency sweep Figure 7 shows the damped, natural frequencies of the first three structural

modes to be 1 6, 2 5 and 3 3 Hz respectively Each of the bending modes has an assumed damping ratio of approximately 0 03, typical damping for aircraft structures Observations reveal that most of the energy of the aeroservoelastic response lies in the first bending mode, which is within the bandwidth of the VMS

The GA was ported from Simulink to C++ using MATLAB's Real-Time Workshop The simulation was then implemented for use in a real-time simulation driving the VMS for piloted studies The simulation was run at 80 Hz while passing position commands to the VMS hardware running at 40 Hz

3.2 Visual Motion Simulator

The simulator used for the piloted simulations was NASA LaRC's Visual Motion Simulator, shown in Figure 9 The VMS is a 6DoF, 60 inch stroke, synergistic motion base simulator The simulator is equipped with CRT displays for out-the-window scenes and multiple programmable, Heads-Down displays A Heads-Up display is superimposed on the visual scenes on the forward, out-the-window CRT and is capable of displaying a wide variety of flight data The VMS utilizes an electronic, two-axis side stick controller with adjustable stick force gradient and damping along with hydraulic rudder pedals (7) The breakout force of the inceptor was approximately 4 lb_f, with a linear force gradient and max deflection limits of +/- 20 degrees
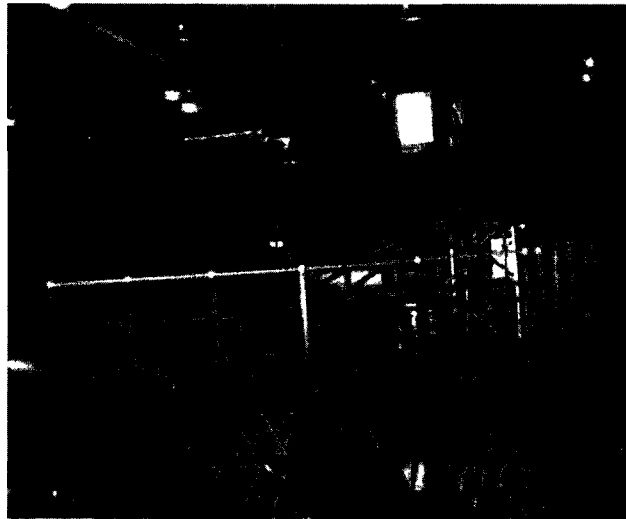
Figure 9 VMS
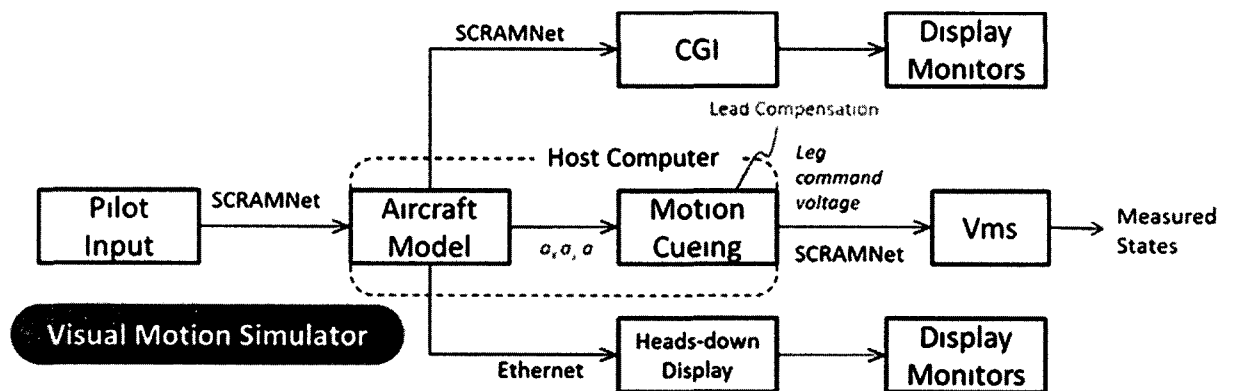
Figure 10 VMS system architecture

As shown in Figure 10, the VMS uses a motion cueing algorithm based on sending motion cues to a pilot's vestibular system that would, in turn, perceive the motion cues as sensed accelerations similar to the actual commanded accelerations going into the cueing algorithm The motion cueing algorithm uses angular orientation cues to help simulate translational acceleration Due to the limited excursion nature of motion base

platforms, the cueing algorithm uses a washout filter to slowly attenuate extended duration commanded accelerations to avoid both position and velocity limits on the platform (8) Thus large, low frequency commanded motions will be attenuated to a greater extent than higher frequency motions However, these low frequency large excursions, which are typically associated with the rigid body motions, have not been shown to contribute to biodynamic coupling Table 2 shows the operational envelope of the VMS

Table 2 : VMS operational envelope

Degree of Freedom	Excursion (in |deg)	Velocity (ips | deg/s)	Acceleration (g | deg/s^2)
Surge	-48 | 49	-24 | 24	-0 6 | +0 6
Sway	-48 | 49	-24 | 25	-0 6 | +0 7
Heave	-30 | 39	-24 | 26	-0 8 | +0 8
Yaw	-32 | 32	-15 | 15	-50 | +50
Pitch	-20 | 30	-15 | 16	-50 | +51
Roll	-22 | 22	-15 | 17	-50 | +52

Reference (9)

The measured frequency response of the VMS to commanded rigid body motion is shown in Figure 11 The measured motion indicates a behavior represented by , with the input representing commanded rigid body acceleration and the output being the actual measured acceleration of the motion base As expected, the approximated transfer function (shown in Figure 12Figure 13) does not precisely match the actual response of the motion base due to nonlinearities in the design of the motion cueing algorithm and simulator hardware

$$G_{VMS_{washout}} = e^{-0.040s} \frac{7.854}{s+7.854}$$ (Eq 1)

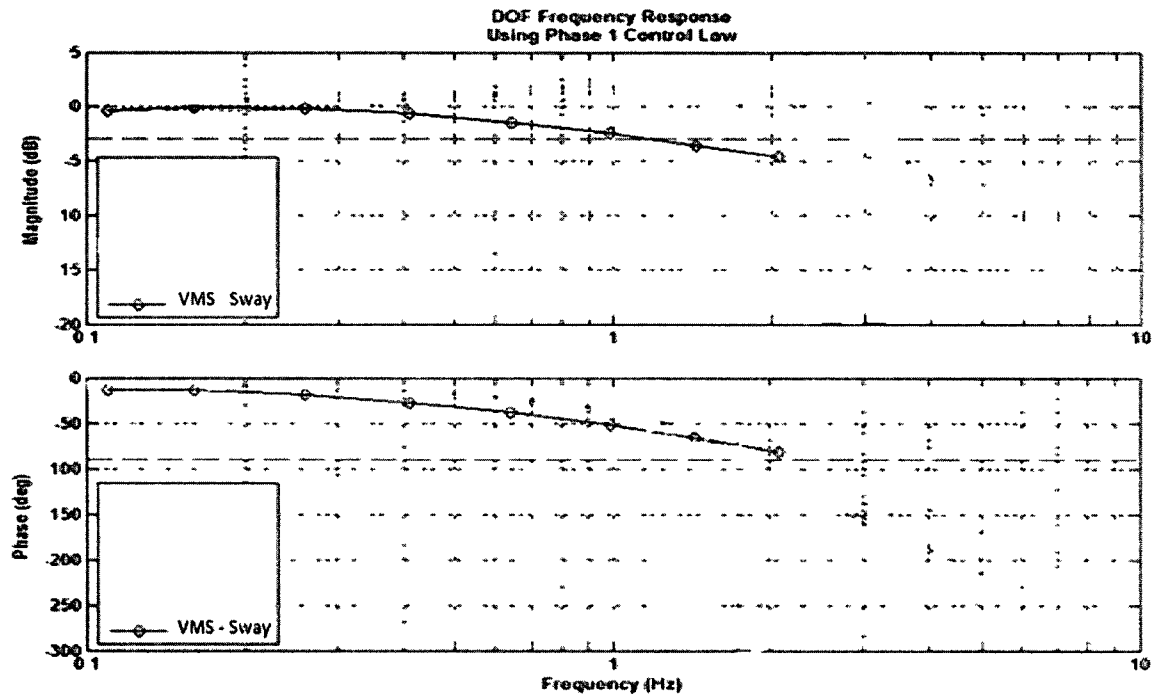**Figure 11 VMS measured bode response – rigid body response**
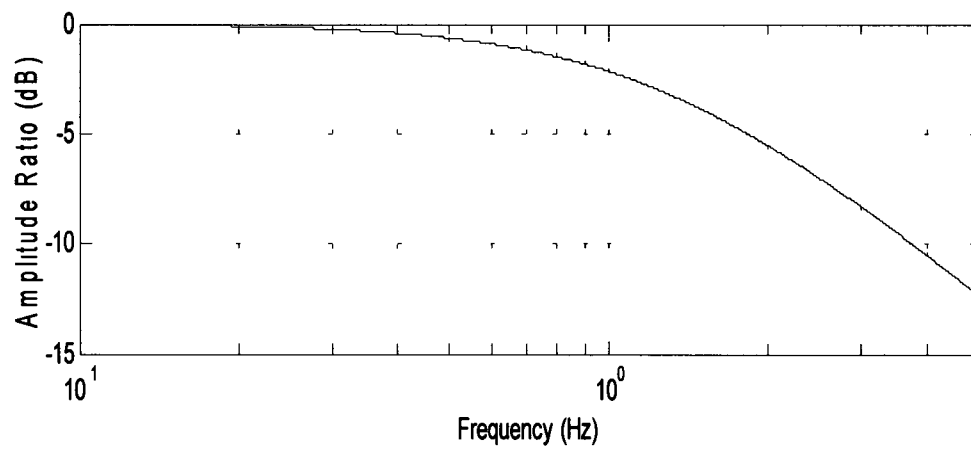

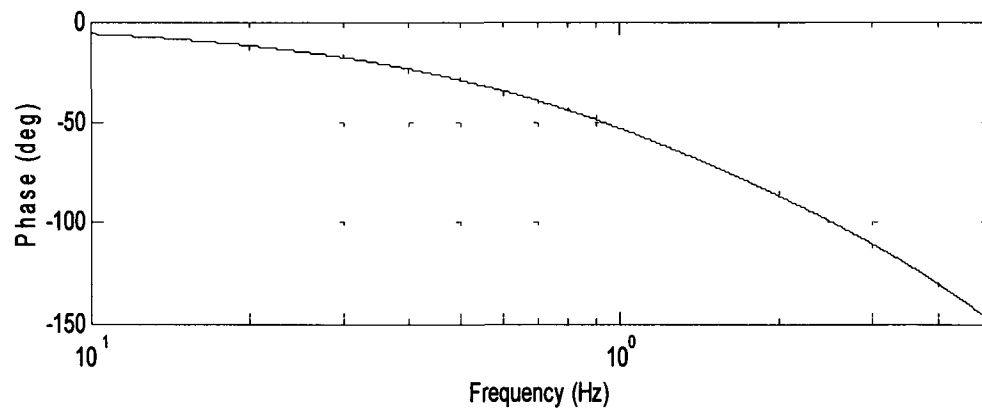**Figure 12 VMS bode plot – amplitude ratio - rigid body motion**

Figure 13 VMS bode plot – phase - rigid body motion

The commanded accelerations from the structural model bypass the washout filter The reason for this implementation is due to the fact that the structural accelerations are of higher frequency and with lower displacement than typical commanded rigid body accelerations This setup was done to prevent the heavy filtering and nonlinearities of the washout filter which would have filtered and eliminated much of the commanded DASE motion The less attenuated, measured frequency response of the commanded-to-measured structural model accelerations is shown below Note that the phase lag does not exceed 90 degrees until approximately 1 5 Hz Figure 14 and Figure 15 show the measured response, along with the model fit to the measured VMS dynamic response data used in the pilot model
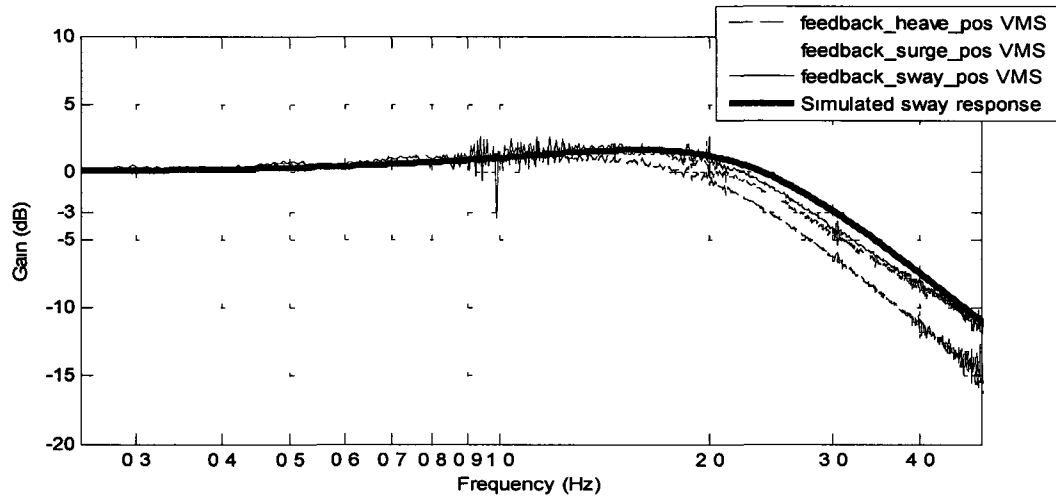
Figure 14 VMS measured vs simulated frequency response – gain
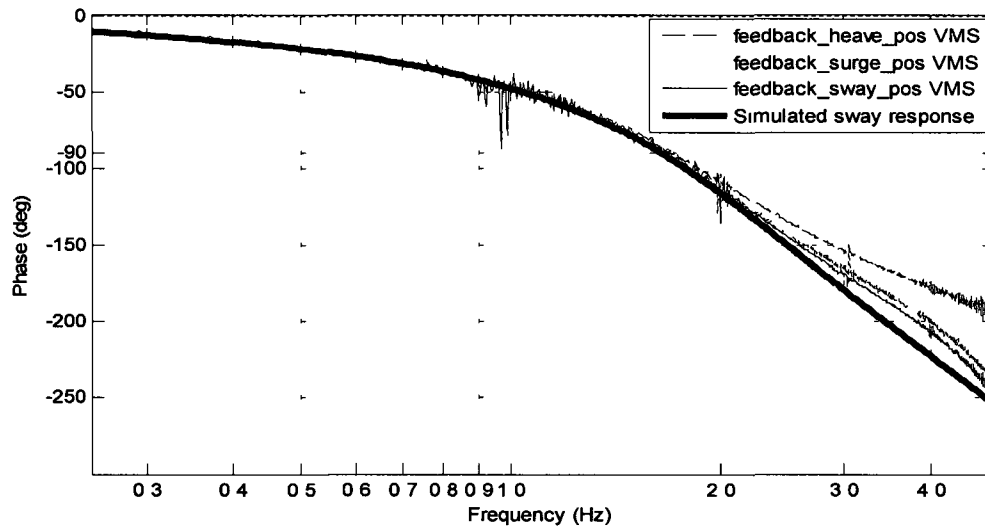
Figure 15 VMS measured vs simulated frequency response – phase

The 'bypass' model of the VMS was modeled with the following transfer function

$$G_{VMS_{bypass\_washout}} = e^{-0\,063s}\frac{245\,3(s+11\,9)}{(s+16\,9)(s+6\,3\pm11\,6\iota)}$$

(Eq 2)

Piloted tasks involving commanded accelerations above 1 5 Hz will cause a growing phase discrepancy between the pilot's visual information and sensed motion base acceleration as the phase lag of the VMS increases to 90 degrees of phase lag and beyond However, piloted sessions that do not require active pilot input (e g subjecting a pilot to an artificially constructed commanded motion base acceleration as described in Chapter 5 are not necessarily limited to 1 5 Hz as long as the measured acceleration of the platform itself is known and used instead of commanded acceleration

4. PILOT MODELING – LITERATURE REVIEW

4.1 Modeling Pilot Control Strategy

The model for the pilot control strategy is based upon previous pilot modeling efforts
Extensive literature exists on modeling pilot control strategy in simple, single-axis
control tasks In these tasks, the human operator receives error information via a display
and minimizes the error through a simple control device (1), (10) Crossover models
have been developed to imitate changes in pilot response with disturbances in the
commanded input frequency to the system shows the general, open-loop form of
McRuer's crossover model in single-loop systems

$$Y_p Y_c (j\omega) = \frac{\omega_c}{j\omega} e^{-j\omega\tau} \qquad \text{(Eq 3)}$$

The plant and the controller in this system are represented by Y_p, Y_c represents the pilot
and controller systems, and ω_c represents the crossover frequency The basic premise of
the crossover model assumes that a human operator's response can be modeled by a
linear function of the visual input, plus some remnant noise not linearly related to the
input (11) The "servo model" nature of the crossover model allows the phase lead or
lag of the simulated human operator response with respect to the input to depend
explicitly on the controlled element dynamics and the crossover frequency of the pilot-
plant system A pilot-plant system represented by a crossover model is hypothesized at
the crossover frequency to have a gain with -20 dB/decade slope Additionally, the input
must be random in nature Experiments validating the crossover model have shown the
remnant to be small in power with respect to the input (12) The basic limitation of
McRuer's crossover model is that it models the combined pilot-system combination

Ronald Hess formulated a human operator model that separates the pilot from the
controlled plant Hess's model, or the structural model, assumes that proprioceptive
feedback of output rate is fed back to the pilot along with output "position" (2) Adding
the proprioceptive feedback loop represents the signal processing nature of a human
operator Being derived from the basic theory of the crossover model, the structural

model also assumes the existence of remnant noise to the pilot response (omitted from Figure 16) Figure 16 below shows the general form of the structural model
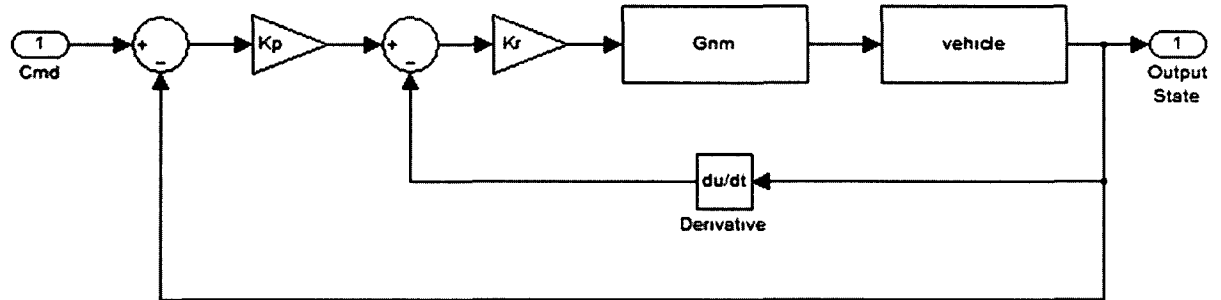

Figure 16   Generic form of structural model

As shown in Figure 16, the structural model provides an explicit form of the pilot separate from the controlled plant The gains K_p and K_r represent gains on the proportional and proprioceptive feedback errors The system G_{nm} represents a 2nd order approximation for neuromuscular lag, where ζ=0 707 and ω = 10 rad/s (13)

$$G_{nm} = \frac{\omega^2}{s^2+2\zeta\omega s+\omega^2}$$

(Eq 4)

The structural model has been applied to multi-loop pursuit control tasks with success in the past (13) The model structure assumes a combination of a number of single-task structural models equivalent to the number of input parameters the pilot is trying to equalize Figure 17, below, demonstrates the result of the process of cascading single input structural models, based on the number of inputs to the pilot, to create a new multi-loop model Assuming two inputs to the pilot, the entire system of Figure 16 is inserted as the new plant of the next structural model In Figure 17, the entire system of

Figure 16 is inserted into the subsystem named "Vehicle with primary-loop closed" This process is repeated for each additional input passed to the human operator
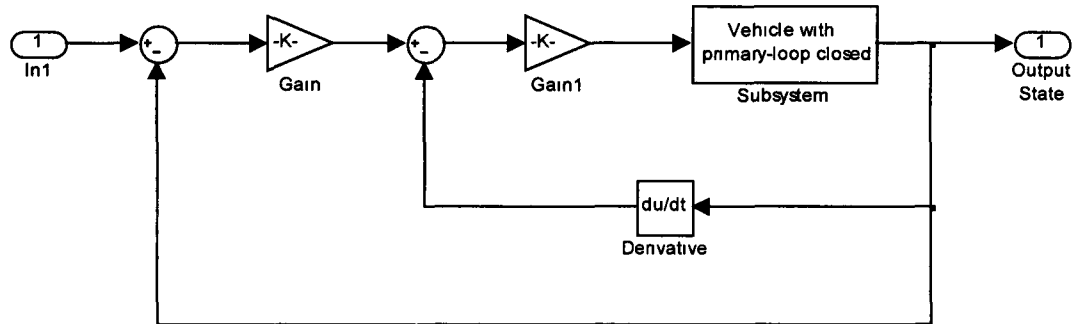

Figure 17 Multi-loop structural model

There are several techniques for determining the gains of a multi-loop structural model Time domain analysis involving the passing of step and sinusoidal inputs to look at the gain, phase and damping nature of the response can be used to estimate an overall level of damping for the pilot-plant system (14) One can also generate the frequency response of the pilot-plant system and adjust the gains until the bandwidth of each successful loop corresponds to what is predicted by traditional crossover modeling theory The gains are chosen to achieve a crossover frequency near 2 rad/s for the innermost loop or single-axis structural model (13) Crossover model theory hypothesizes that the gains in each successive loop should be specified to achieve a 1/3 reduction in open loop crossover frequency (12) An additional benefit of using the structural model is the ability to correlate the power of the proprioceptive feedback relative to the proportional feedback to assess vehicle handling qualities (13)

4.2 Modeling Physiological Response

Biodynamic coupling is dependent not only on pilot control strategy but also involuntary feedthrough resulting from aeroelastic accelerations at the pilot station This structural motion feeds through the pilot's body and into the stick This component of the control input can drive the aircraft dynamics at the resonant frequencies of the airframe structure which could lead to growing aeroelastic accelerations at the pilot station

Various biomechanical models for human pilots have been previously derived to evaluate the impact of vibration Researchers at Systems Technology, Inc successfully constructed a model consisting of masses, springs, and dashpots to model the feedthrough of vertical vibrations at the pilot station to longitudinal stick inputs of several pilots (15) However, this model was not used in conjunction with a model that could predict pilot control strategy and thus present a closed-loop biodynamic coupling analysis

Researchers have also applied traditional crossover modeling theory to the biodynamic coupling phenomenon Researchers at Stanford University and the Israel Institute of Technology performed a piloted simulation study using a simplified, first order plant to drive a motion base simulator (16) They modeled the human operator with the precision model with the basic structure shown in

$$Y_p(j\omega) = K_p \frac{e^{-j\omega\tau}}{j\omega T_N + 1} \frac{j\omega T_L + 1}{j\omega T_I + 1} \qquad \text{(Eq 5)}$$

The precision model gives an explicit representation of the pilot separate from the plant The model includes equalization constants for lead (T_L) and lag (T_I), defines a general time delay ($e^{-j\omega\tau}$), and typically includes a first order neuromuscular lag (T_N) (12) Using a simple plant (K_c/s), researchers were able to obtain a good match for the human operator control in a single axis tracking task An "open loop" experiment was performed subjecting the pilot to accelerations not related to the pilot output The magnitude of the biodynamic feedthrough was experimentally demonstrated to behave

similar to a band-pass filter (16) In their approach, however, the researchers assumed a negligible phase lag between the pilot station accelerations and the involuntary feedthrough in the region of interest Experimental data obtained from the Ref-H and SDSS piloted simulation studies demonstrated an appreciable phase difference between accelerations at the pilot station and feedthrough to the stick This phase difference will be very important when analyzing the entire closed-loop pilot-airplane system Figure 18, below, shows a portion of a time history with evidence of biodynamic coupling from the SDSS study The experiment demonstrates noticeable phase difference between the sinusoidal aeroelastic motion of the motion base and apparent similar-frequency response of the biodynamic feedthrough in the measured stick motion
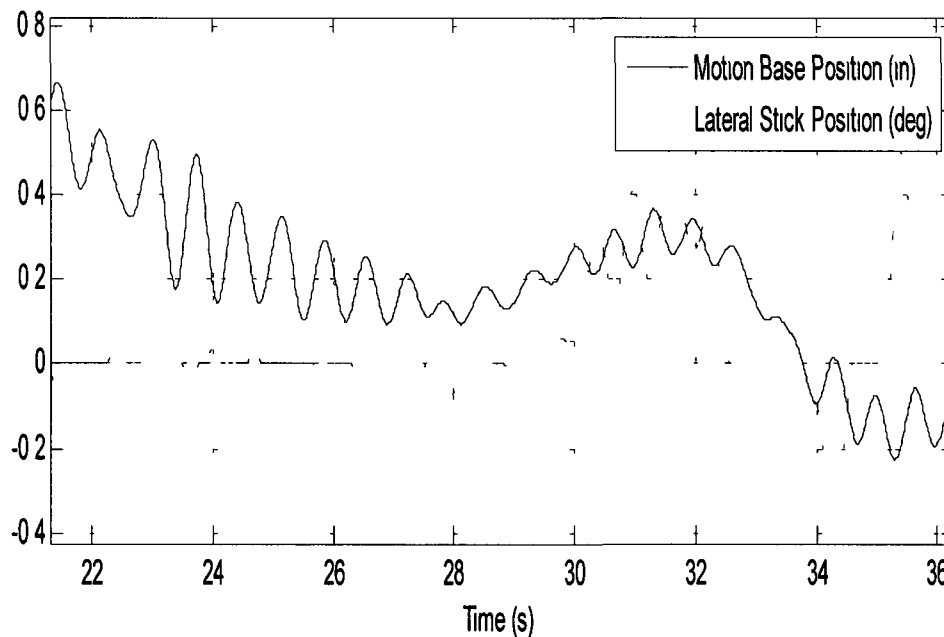
Figure 18 Stick deflection vs motion base position

Thus, a model capturing the magnitude and phase relationship between the aeroelastic motion and the resulting feedthrough to the stick is needed Small changes in phase in a

single component of the pilot-airplane-simulator system will be shown to have a large impact in the resulting biodynamic coupling

5. PILOT STUDY FOR SPECTRAL ANALYSIS OF PILOT STATION ACCELERATIONS TO STICK FEEDTHROUGH

A piloted study was performed to capture the relationship between lateral motion base acceleration and feedthrough to isolate the biodynamic feedthrough from cognitive control response This study was done with the assumption that the physical, involuntary feedthrough of aeroelastic accelerations to the stick is uncorrelated with pilot control strategy The resultant system represents the biomechanical response of the pilot to lateral accelerations coupled with the inceptor dynamics

During the experiment, the test pilot was instructed to hold the inceptor at a constant deflection whilst being subjected to a frequency sweep of lateral motion base acceleration The resulting motion base acceleration and stick position were recorded and treated as input and output signals, respectively, for system identification for the physiological model The results from one pilot were used to create the physiological model from this process

The repeatability in biodynamic response between runs for a single pilot is demonstrated by Figure 19, showing the recorded stick deflection from two separate runs with identical commanded motion base accelerations Both runs were performed by the same pilot
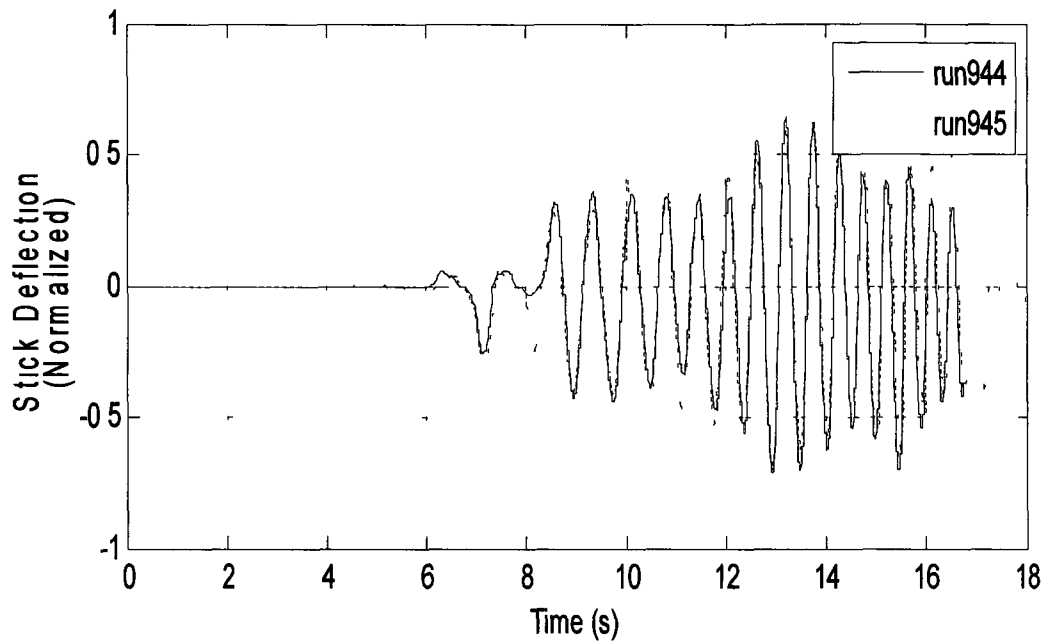
Figure 19   Experiment repeatability, stick deflection from similar runs

Figure 20 and Figure 21 show the time domain response of lateral stick deflection and its second derivative excited by motion base acceleration in the form of a sine wave of linearly increasing frequency The frequency content ranges from 0 5 Hz to 3 Hz

Observe that at lower frequency there is little to no feedthrough to the stick This is most likely due to pilots able to anticipate and counteract lower frequency accelerations
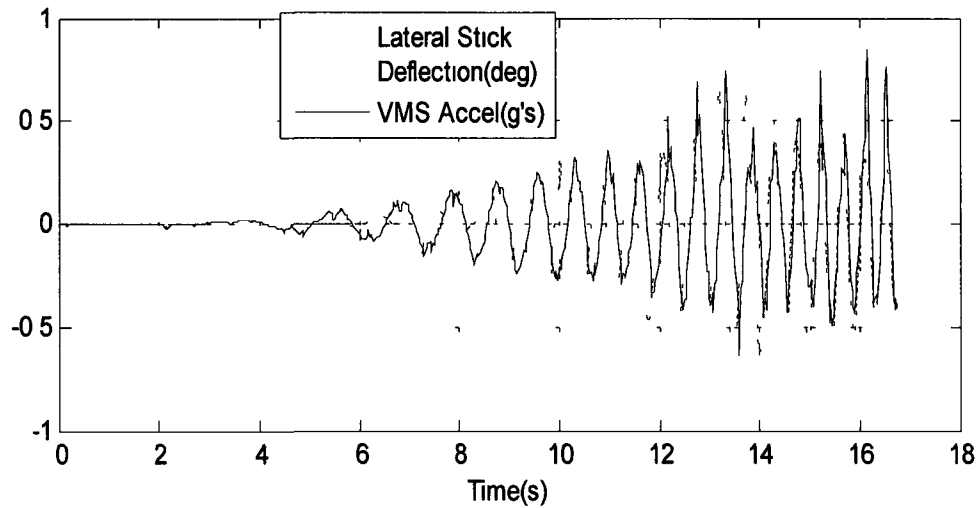
Figure 20   Involuntary feedthrough – lateral acceleration to stick position
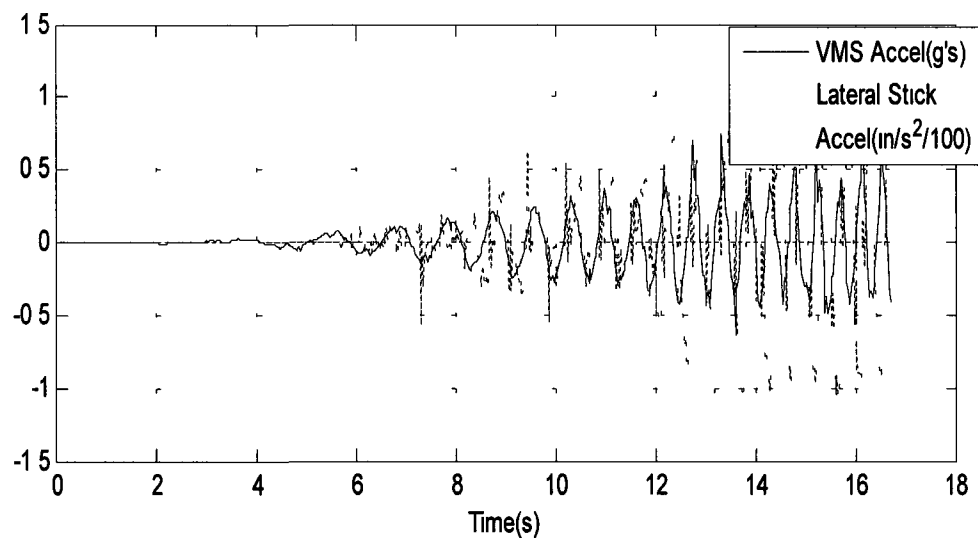

Figure 21   Involuntary feedthrough – lateral acceleration to stick acceleration

The second derivative of the lateral stick deflection shows a response of similar frequency content of that of the motion base with a phase shift and gain   Plotting lateral stick acceleration this time shows the actual amount of lag between motion base acceleration and lateral stick acceleration   Analysis of these signals in phase space will

give a clearer picture of how much phase lag at each frequency is present Figure 22 -
Figure 24 show a collection of time histories in phase space, again with motion base
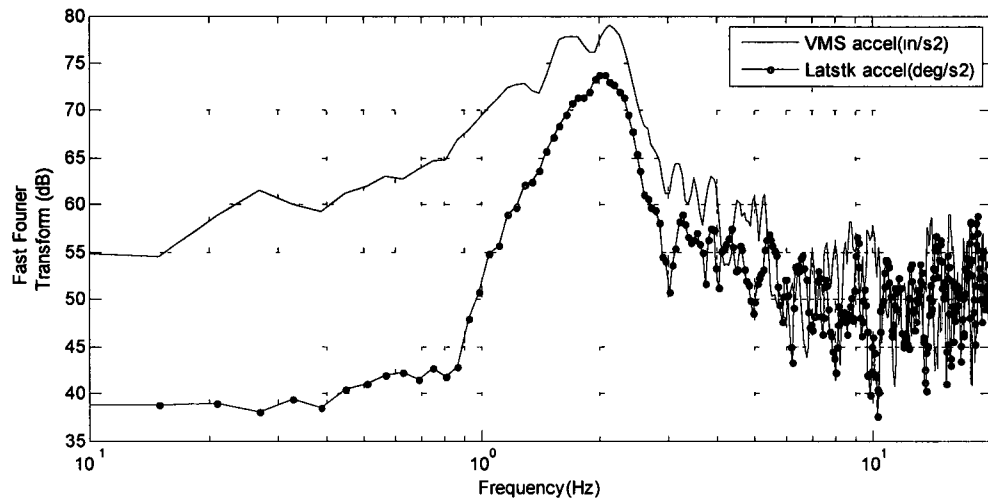acceleration as the system "input" and lateral stick acceleration as the system "output"

Figure 22 Frequency content of motion base acceleration and resulting lateral stick acceleration
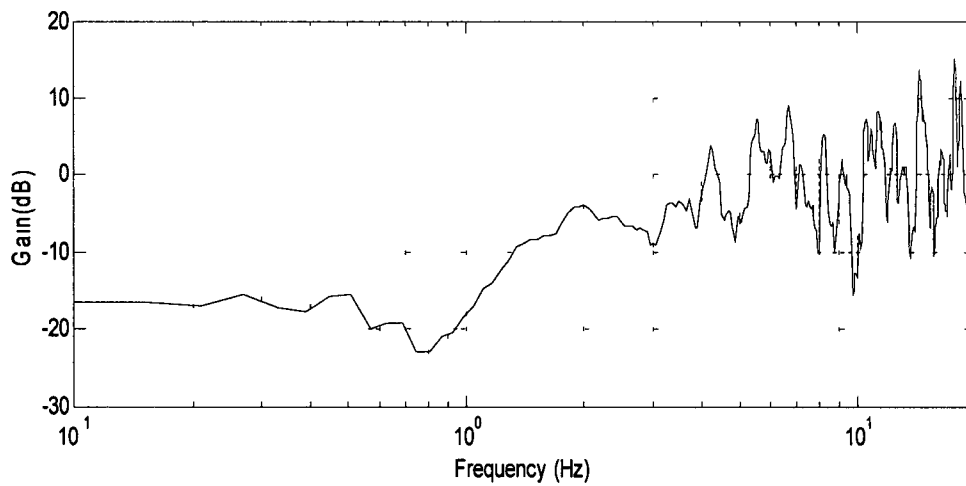

Figure 23 Amplitude ratio of VMS acceleration (in/s^2) to lateral stick acceleration (deg/s^2)
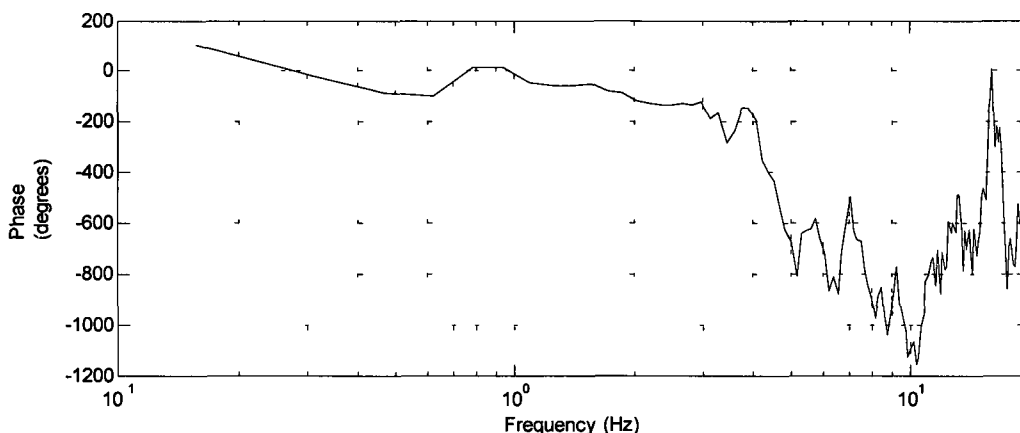
Figure 24   Phase lag of VMS acceleration to lateral stick acceleration

The majority of the energy of the acceleration of the motion base was approximately between 0 75 and 2 5 Hz The response of the lateral stick shares similar frequency content, but the gain on the output at the lower range of frequency is significantly lower, possibly demonstrating that at lower frequencies, pilots are able to predict and limit the amount of biodynamic feedthrough This hypothesis was predicted and seen experimentally in a previous study (16) The model thus far will represent the physiological response across the spectrum of testable accelerations

The data suggest that with a limited frequency range of interest, the biodynamic feedthrough can be modeled with a linear, time-invariant model As hypothesized and experimentally suggested the lower range of frequency will be attenuated up until 0 75 Hz The upper range of frequency will be practically limited to 3 Hz as a result of limitations in VMS bandwidth However, this is not a significant limitation because the majority of power of the piloted inputs appears to be less than 1 Hz Figure 25 and Figure 26 show pilot lateral stick inputs from four different pilots performing the standard lateral offset task The latter shows the power of the recorded inputs, indicating that the bandwidth of the pilot control responses appear to be less than 1 Hz when flying with a rigid-body aircraft response model
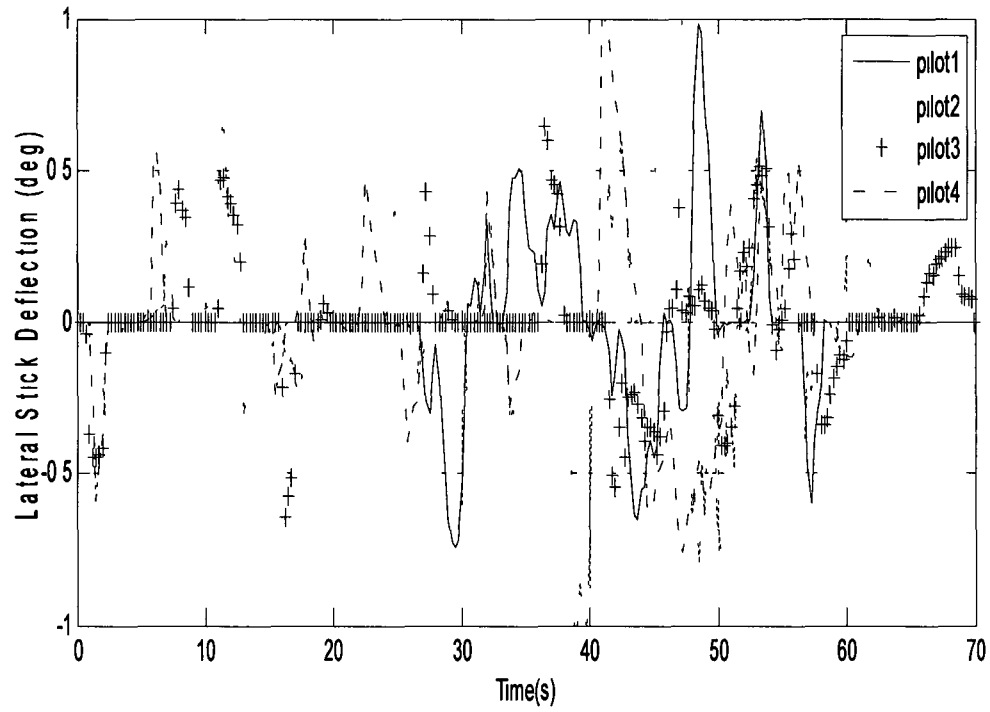
Figure 25   Collection of recorded stick time histories from various pilots
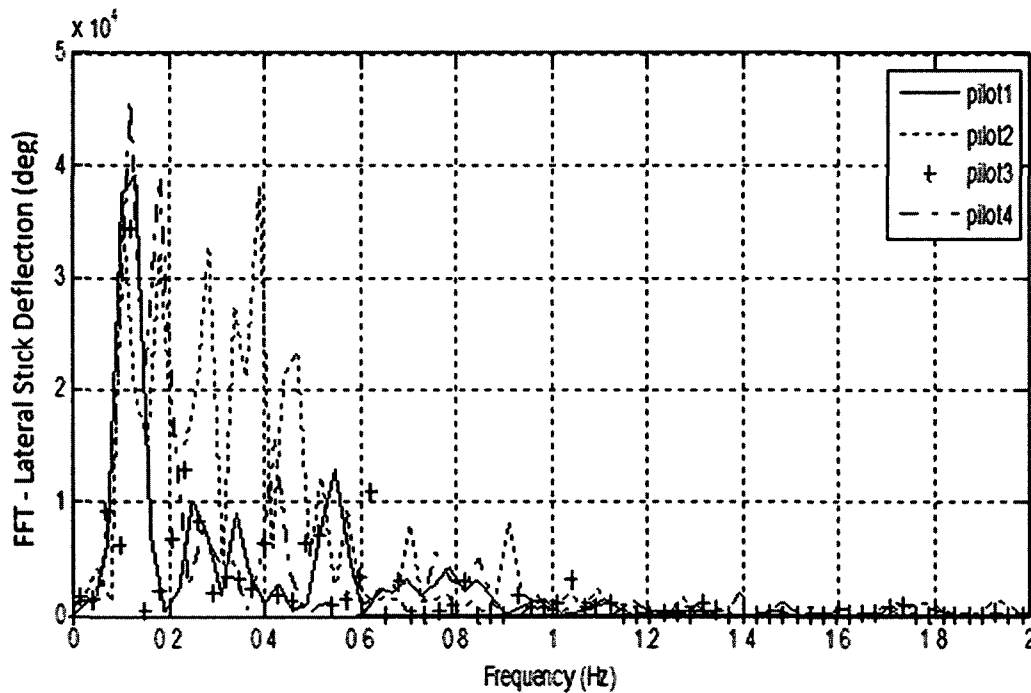
Figure 26   Power of recorded pilot inputs

The actual frequency content of the expected pilot station accelerations will be dependent not only on the pilot control strategy, but also on the airplane rigid body dynamics and the structural modes The results suggest that the majority of the energy inputs due to pilot control strategy will be at frequencies lower than 1 Hz, while the involuntary feedthrough will be attenuated at frequencies lower than 1 Hz

The appreciable phase lag between input and output of this involuntary system also suggests that, when placed in parallel with the model for pilot control strategy, changes in phase of any of the individual components of the pilot-airplane-system may impact the overall level of predicted biodynamic coupling

6. PILOT MODEL

6.1 Bio-Feedthrough Model

A mathematical model representing the involuntary feedthrough to the stick was created from the previously mentioned experimental data A generic, linear, time-invariant (LTI), 5th order transfer function was fit to the raw motion base acceleration to lateral stick response data The transfer function is of the form

$$G_{involuntary_{feedthrough}} = \frac{-4\ 44e^{-2}z^2 + 3\ 29e^{-5}z}{z^5 - 1\ 88z^4 + 0\ 766z^3 + 0\ 434z^2 - 0\ 248z - 1\ 49e^{-2}}$$ (Eq 6)

This simulated approximation represents the transfer function fit from motion base acceleration to lateral stick position The transfer function shown in is in discrete-time form because this was the actual form used in the pilot model and used to generate the results to be shown in Chapter 7 The use of lateral stick position as the output instead of lateral stick acceleration was chosen because of the nature of the required output for simulation Experimental data suggest that there is a sharp rise in feedthrough in the middle of the frequency range of interest (Figure 27) Also, as seen from Figure 26, the vast majority of the pilot control strategy, and thus airplane motion, will be in the region that is sharply attenuated Modeling motion base acceleration to lateral stick position closely captures the rigid body, lower frequency attenuation from P S acceleration to stick acceleration inherently in the system identification process, while closely achieving the same gain and phase relationship in the testable frequency range
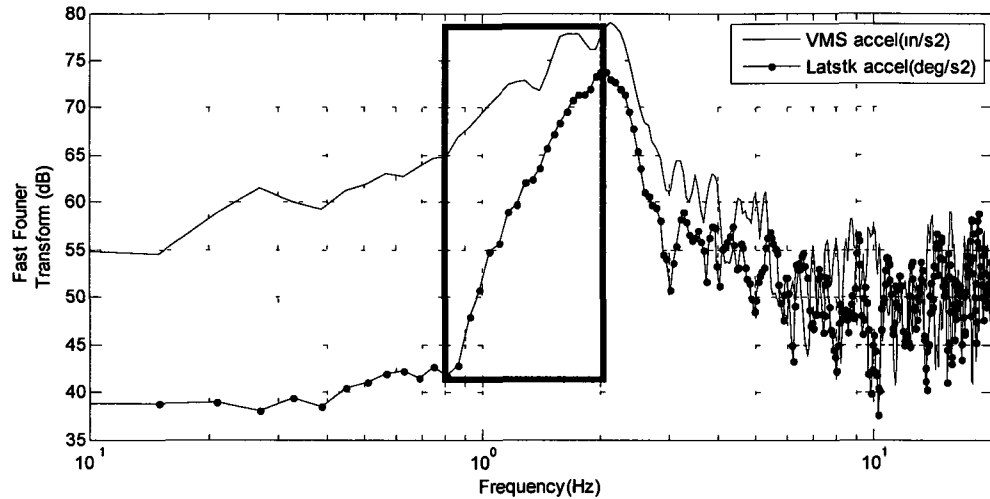
Figure 27 Sharp increase in amplitude ratio

Comparing the LTI system approximation with the time domain response recorded while subjecting a pilot to lateral accelerations shows (shown in Figure 28) an excellent match for a limited frequency range. The gain and phase relationships are captured while the lower frequency response is noticeably attenuated.
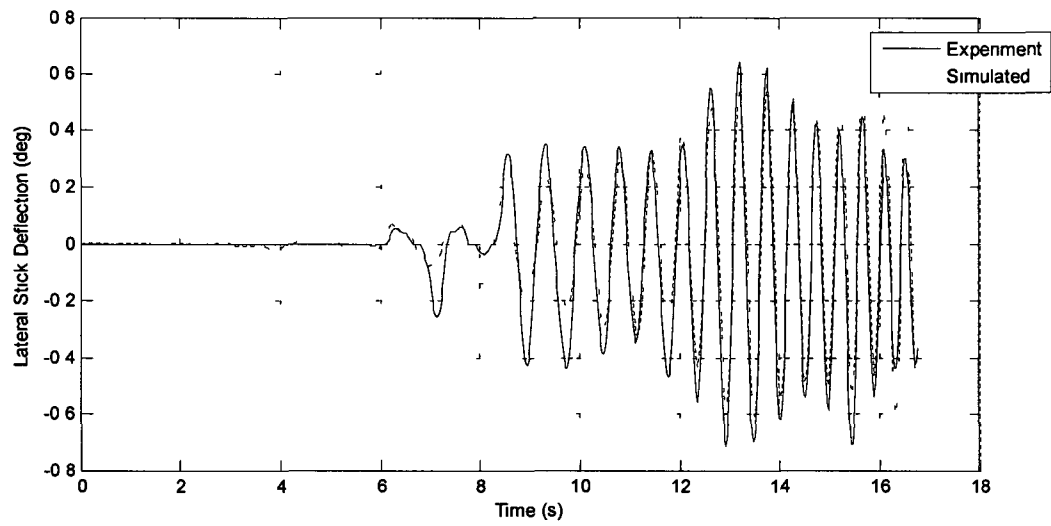
Figure 28   Measured and simulated output

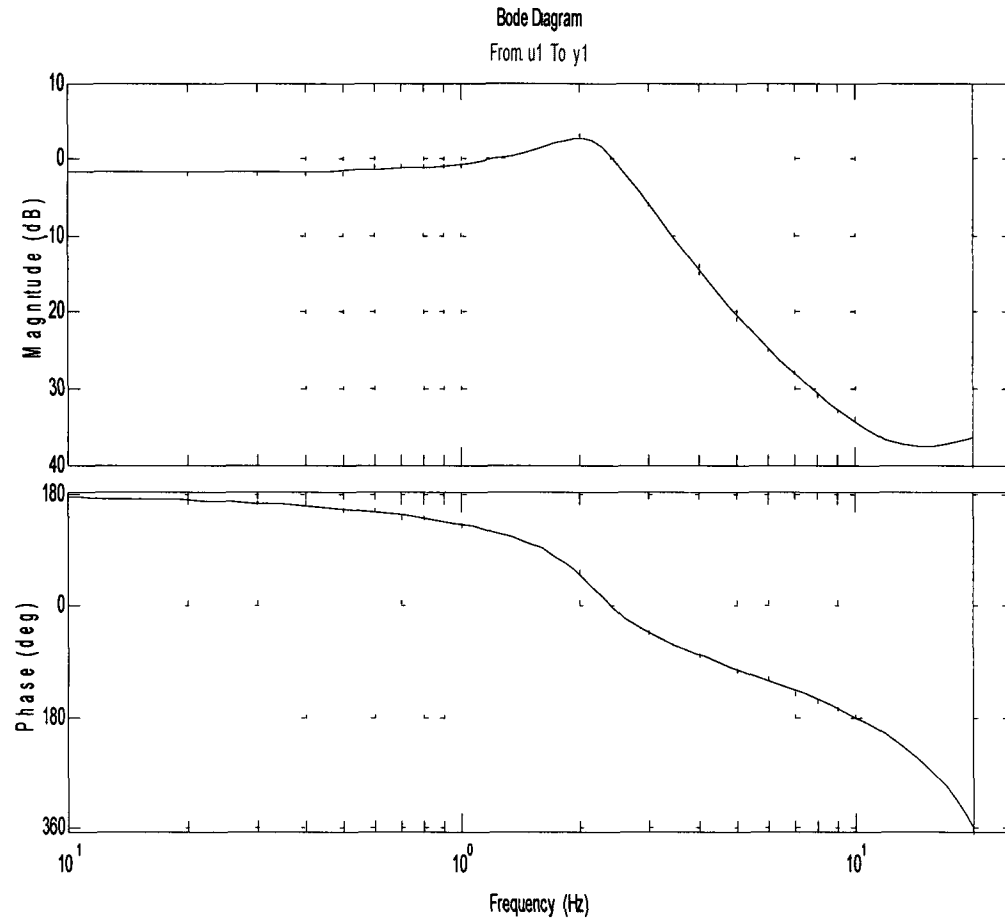Figure 29 shows the bode response of the approximated LTI system

Figure 29 Frequency response of physiological model, units – stick deflection (degrees) per unit acceleration of the motion base (in/s^2)

The discrete time system of was implemented in the final simulation, however, for reference, a continuous time representation is presented in A comparison of the two systems is shown in Figure 30

$$G_{involuntary\_feedthrough_{continuous}} = \frac{-0\ 9102(s+115\ 7)(s+29\ 19)(s^2+88\ 23s+2712)}{(s+115\ 7)(s+29\ 9)(s+15\ 87)(s^2+6\ 734s+186\ 7)} \quad \text{(Eq 7)}$$
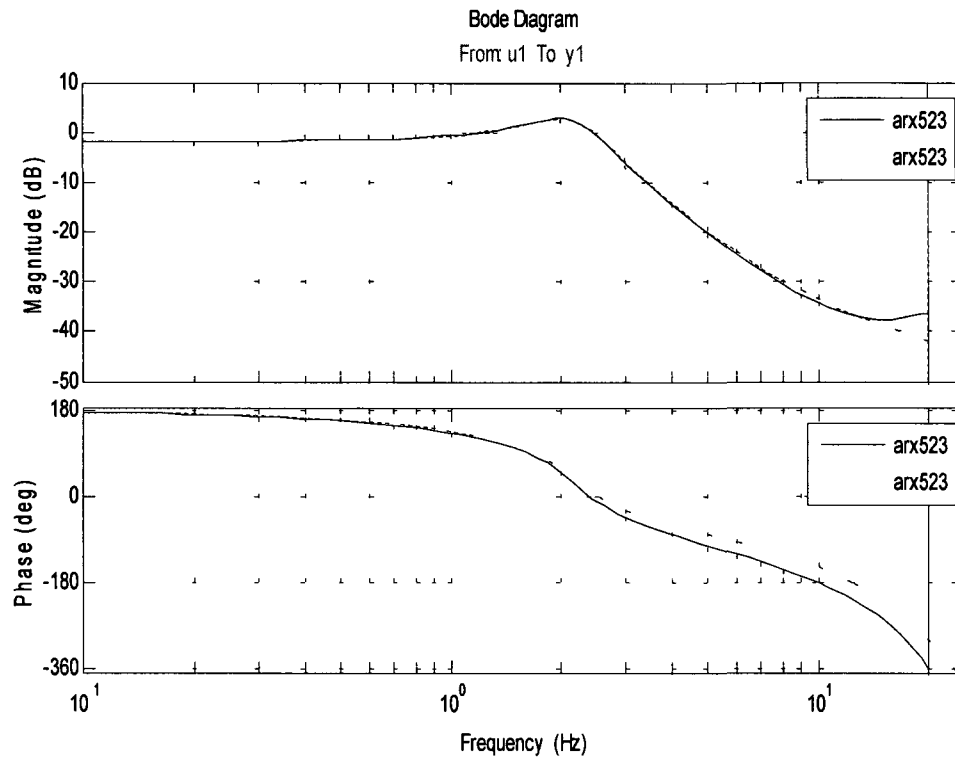
Bode Diagram
From u1 To y1

Figure 30 Biomechanical continuous and discrete time representations, units – stick deflection (degrees) per unit acceleration of the motion base (in/s^2)

The gain of the response of the approximated system falls off after approximately 3 Hz, which, as previously stated, is outside of the frequency range of interest or testable frequency range The input/output phase relationship shows 180 degrees of phase lag (shifted by +360 deg) as a result of the fact that the output is position rather than acceleration The step response of the system is shown in Figure 31, indicating the overall damping ratio in the physiological response to be approximately 0 3 The physiological model will be combined in parallel with the structural model to be described in the following section
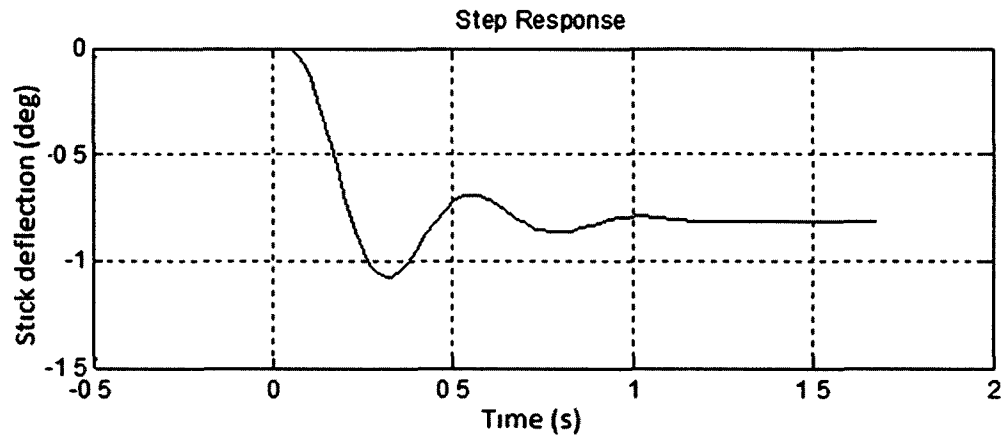
Figure 31   Step response of LTI system

6.2 Crossover Model

The implemented structural model borrows the basic form from Hess's multi-loop structural model Each loop of the structural model contains feedback loops of one of the sources of feedback to the pilot To perform a standard lateral offset maneuver, the pilots generally roll to acquire a bank angle, and hold the bank angle constant until the desired turn rate is achieved The turn rate is held until a desired change in heading (or track angle) is achieved The new heading is then held until the new lateral offset is approximately attained Thus the three feedback parameters in the pilot model are lateral offset position error, bank angle, and track angle The overall structure of the pilot model is shown in Figure 32 with the outermost loop highlighted and the other loops embedded

Figure 32 Crossover model, outermost loop

39
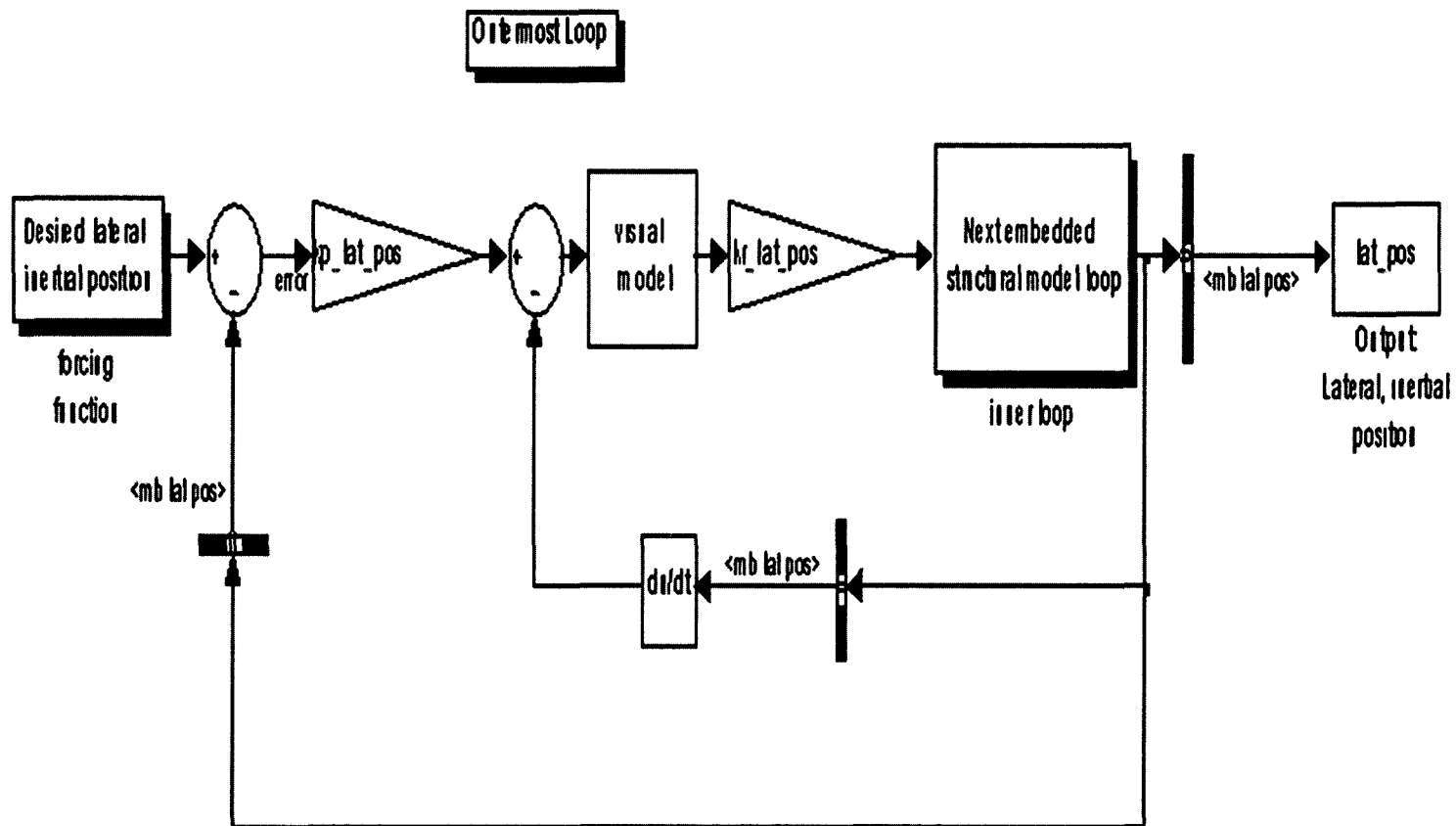
As previously mentioned, the multi-loop structural model is created by taking a single input structural model and replacing its plant with an additional structural model, representing the next input parameter perceived by the human operator The outermost feedback and thus the primary feedback parameter is lateral offset position The second input parameter to the pilot is track angle, and correspondent with the theory for constructing a multi-loop structural model, the "plant" of the outer loop is replaced with another structural model with track angle as the feedback parameter Thus, in Figure 32, the system labeled "inner loop" is actually the next embedded structural loop, shown in Figure 33

Figure 33   Crossover model, Intermediate loop

41
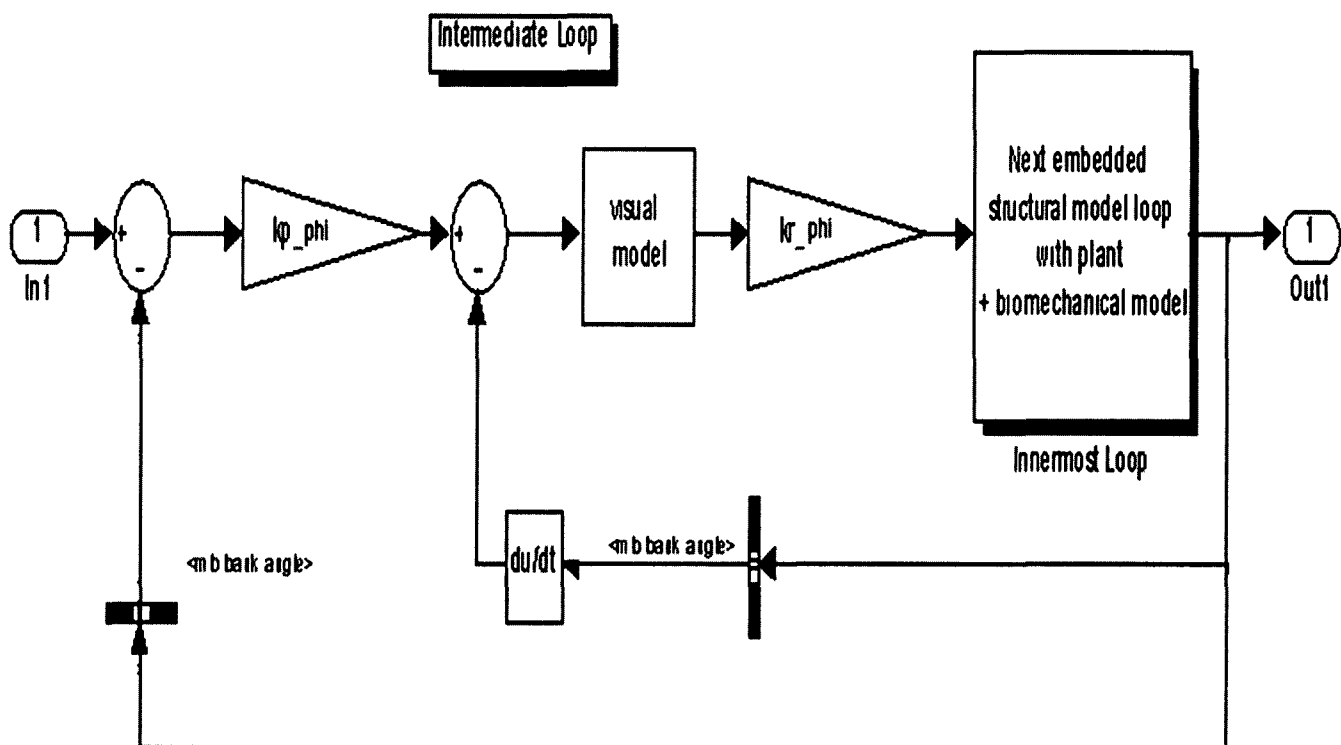
Similarly, the third and final structural model loop is implemented in the same fashion In Figure 33, the system labeled "innermost loop" contains the final structural model loop shown in Figure 34 which is primary controlling bank angle

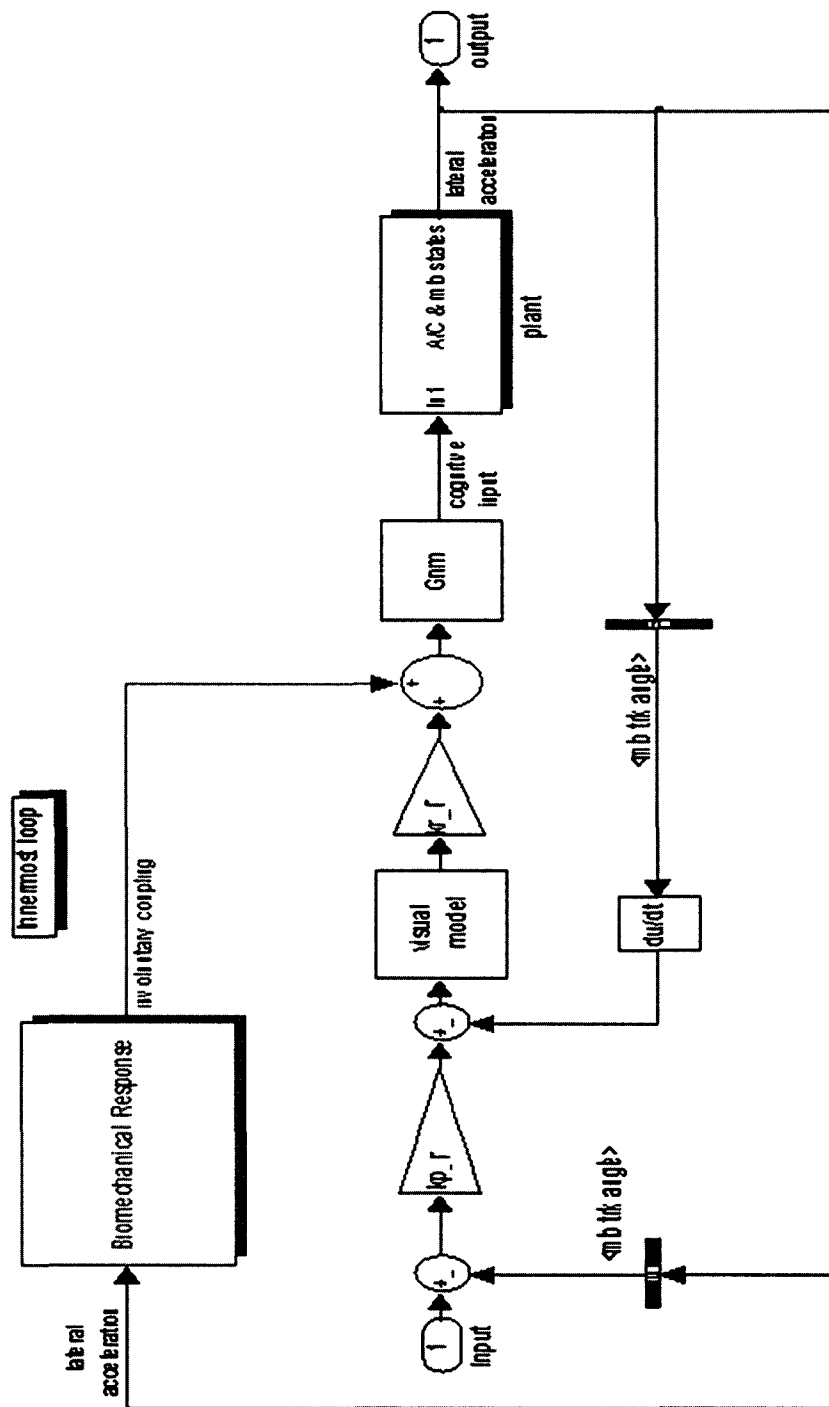

Figure 34 Crossover model, innermost loop

The innermost loop of the crossover model resembles the basic form of a single input structural model, with the plant in series with the feedback loop(s) The plant consists of the Generic Airplane rigid body and structural dynamics, and a model for the VMS A neuromotor model in the form of a second order lag and based on empirical data (14) is applied downstream of the predicted output from the crossover model

The physiological model is added in parallel to the crossover model, upstream of the neuromotor model This implementation presumes the existence of purely involuntary feedthrough independent of the pilot's cognitive response, an assumption made in a previous study with success (16)

In addition to the basic feedback loop structures, there are visual models for the pilot Figure 35 illustrates the structure of the visual cue model
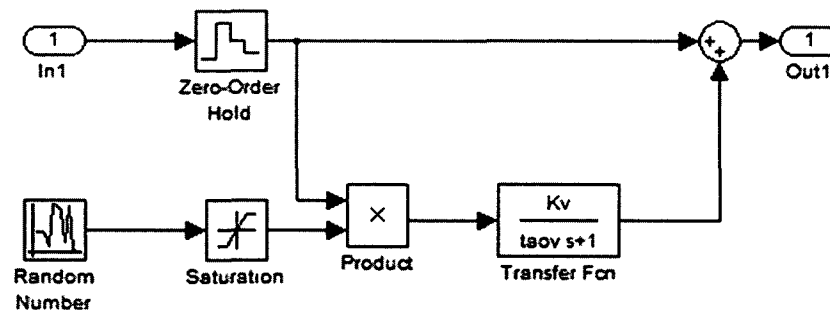

Figure 35 Pilot visual cue

This visual cue adds a lag and injects a small element of randomness into the pilots' visual inputs The locations of the visual models are shown in Figure 32-Figure 34 This model has been used in the past with success in similar piloted studies (13, 14, 17)

For each pilot, the aggressiveness for which each task is performed and the pilot tendencies depend on the size of the lateral offset and time-to-go specified to the pilot

The differences of aggressiveness between pilots stem from a variety of sources including, but not limited to overall pilot aggressiveness, training, state of alertness, and adaptation to aeroelastic accelerations This study will focus on matching the results from a single pilot

7. RESULTS/ANALYSIS

The crossover model was constructed with empirical data from piloted runs A subset of these piloted runs performed without any structural motion will be used for comparison to the simulated model All three of the piloted runs were consecutively flown by the same pilot with an initial lateral offset

To achieve a matching control response the crossover model was fed the same commanded lateral offsets that the pilot sees in the real-time simulation The sluggish (or highly damped) response of the Generic Airplane from lateral stick commands to lateral inertial position resulted in specification of the feedback gains based on time histories from the SDSS study The gains used in the model are shown in

Table 3

Table 3: Crossover model gains

	Lateral Position Error	Track Angle	Bank Angle
K_p	32 9538 (s^{-1})	600 (s^{-1})	5 56E-05 (s^{-1})
K_r	8 10E-04 (deg-s/ft)	290 (deg-s/deg)	0 018 (normalized stick deflection-s/deg)

Figure 36 demonstrates the relative match between a sample of actual pilot inputs and the predicted pilot control response from the crossover model This system matching includes not only predicted control response, but modeled neuromotor lag and motion base dynamics

Figure 36-Figure 39 compare time histories of the states and performance parameters of the simulated model to those of the piloted runs Figure 36 displays a comparison of the

resulting lateral stick deflection of the crossover model and the piloted runs The remaining figures show the changes in the three primary feedback parameters
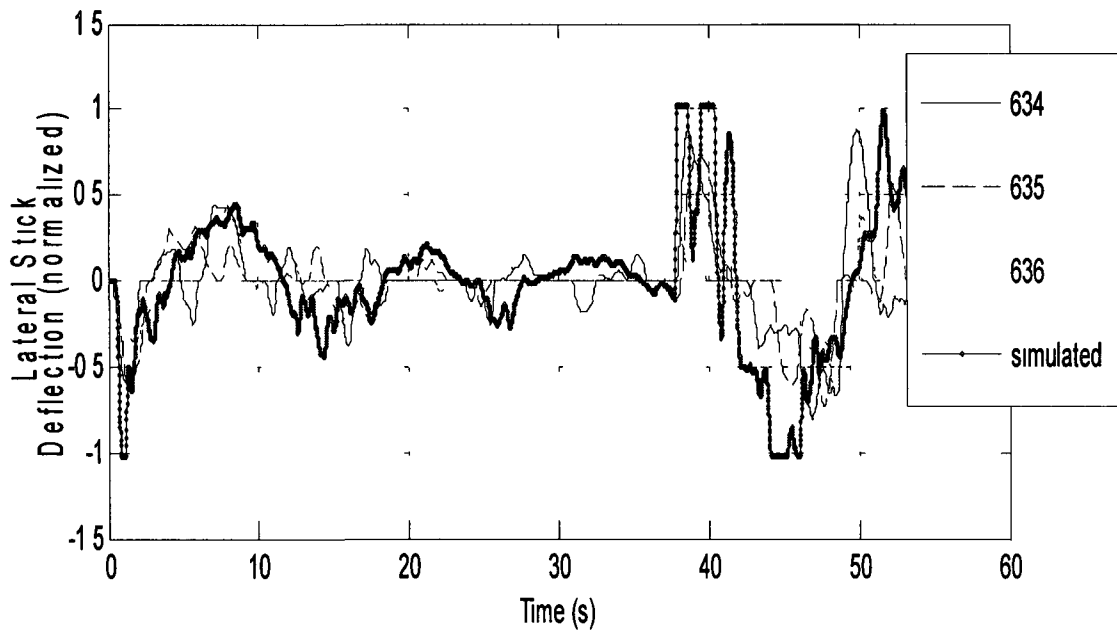

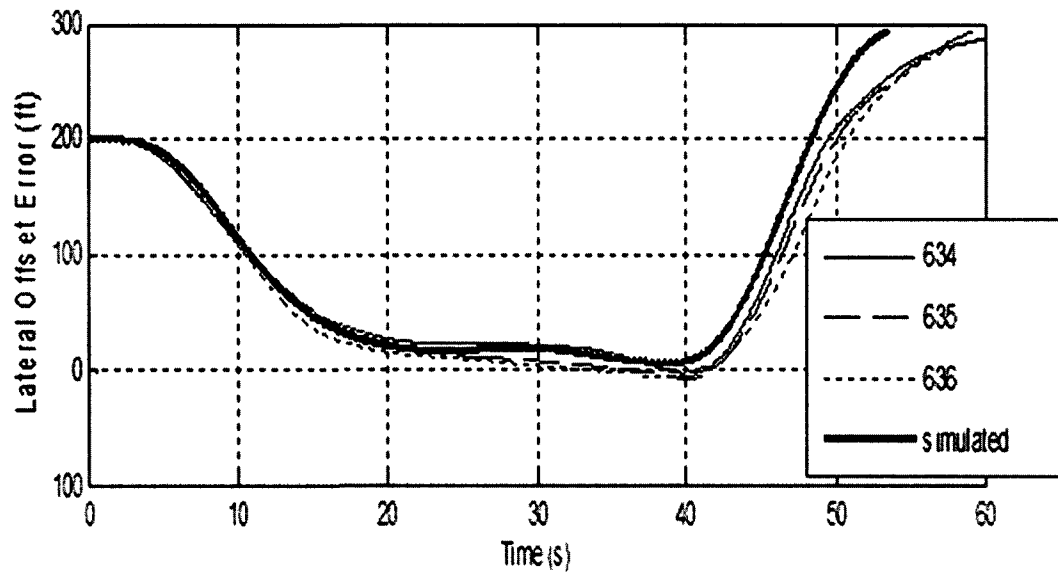**Figure 36 Crossover model vs empirical pilot - lateral stick deflection**

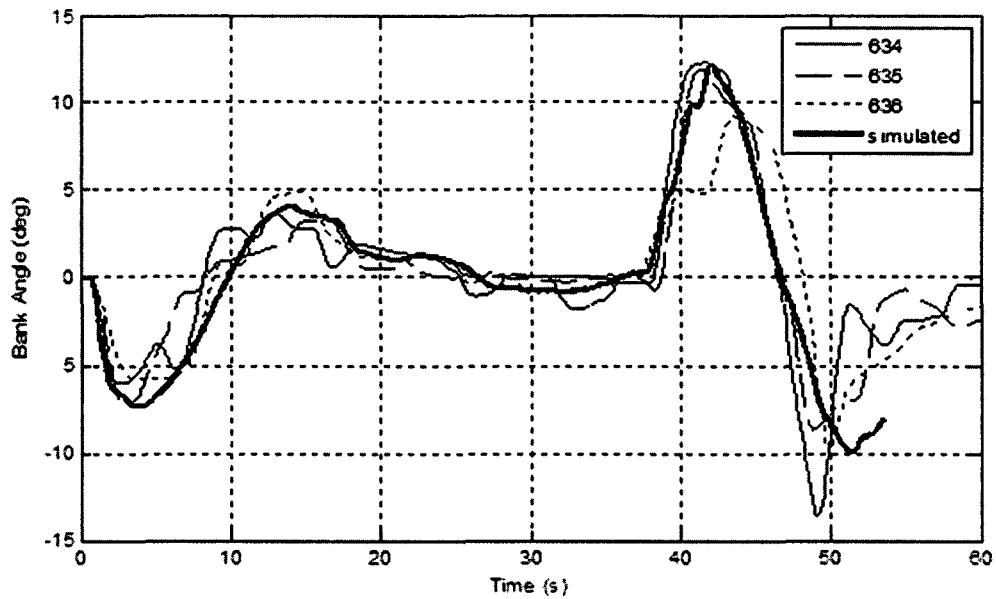**Figure 37 Crossover model vs empirical pilot - lateral offset error**

Figure 38 Crossover model vs empirical model - bank angle
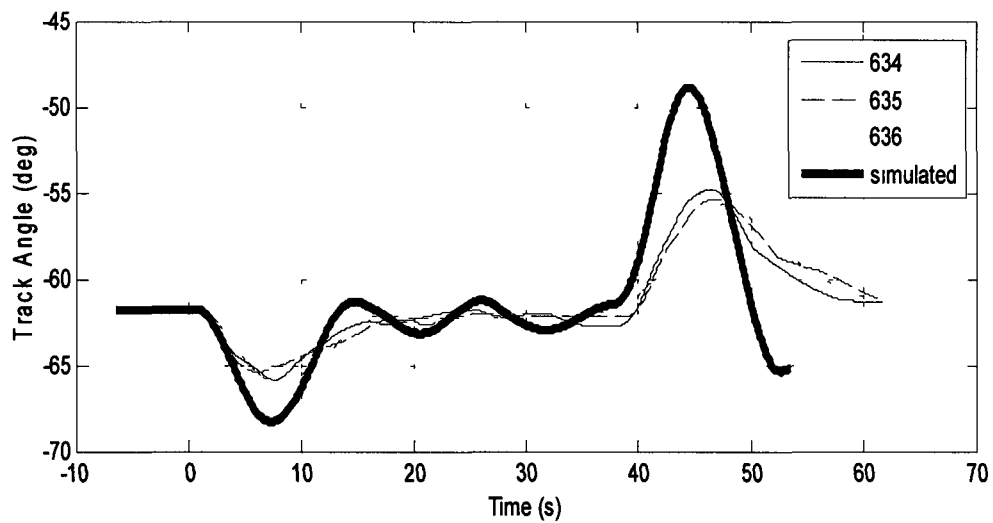

Figure 39 Crossover model vs empirical pilot - track angle

Figure 37 demonstrates the excellent match between simulated and actual pilot

performances of the primary task parameter (lateral offset position) While the bank

angle is also matched very well (Figure 38), the simulated and measured control strategies for tracking heading angle (Figure 39) diverge slightly near the end of the task, although still maintaining similar overall characteristics However, the large yaw rates and overshoots in track angle indicate that the simulated pilot model is a little more aggressive in its control strategy

One way to compare the magnitude response of the stick deflection while "filtering" some of the phase shifting is to integrate the lateral stick position signals Figure 40 shows the similarity in the overall trend of the simulated versus measured pilot responses Along with the discrepancy in pursuing track angle, Figure 40 also suggests the possibility of the simulation using 'more' lateral stick to control lateral offset position
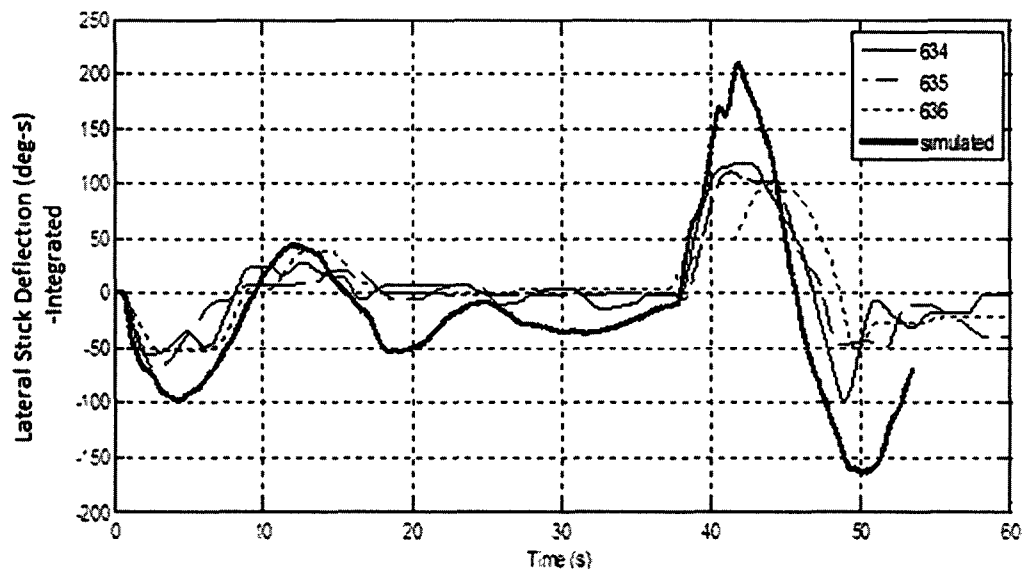

Figure 40 Crossover model vs empirical pilot - integrated lateral stick deflection

Figure 41, as expected, shows that the majority of the frequency content of the crossover model is in the lower end of the frequency range of interest, similar to what is seen in the pilots' control response The frequency content of the simulated model is

also distributed more evenly than that of the measured pilot responses in Figure 26
Targeting a specific peak response frequency for the simulated model was not given
high priority when compared with the response peaks in the measured pilot responses
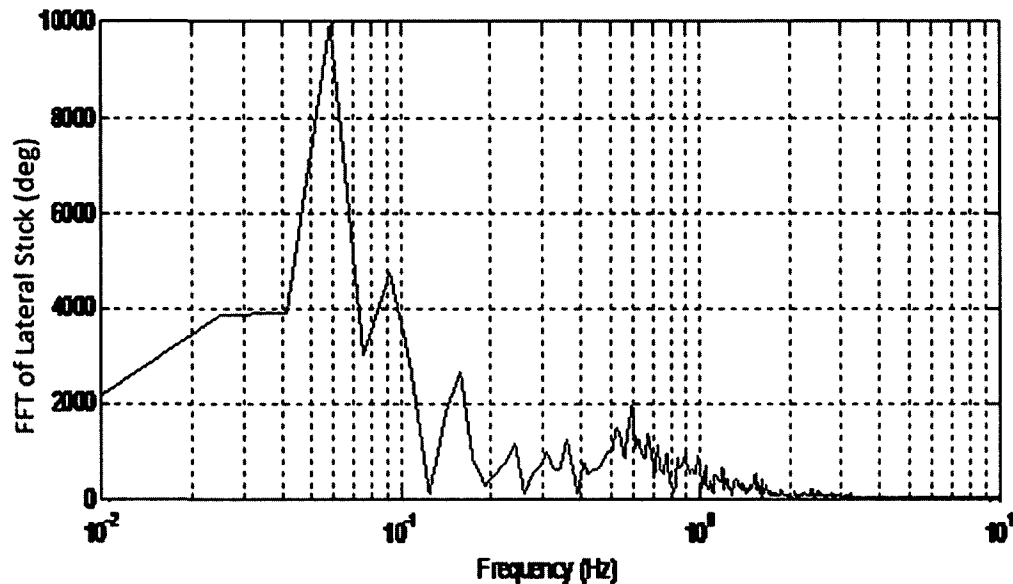vary themselves

Figure 41 Frequency content of crossover model

This resulting crossover model can be used with the previously derived physiological,
airplane, and motion base models to simulate the entire pilot-airplane-simulator
system

7.1 Pilot Model – Biodynamic Coupling

The entire closed-loop biodynamic coupling system can be studied with models of the
pilot control strategy, involuntary response and the aero-environment – in this case, a
generic airplane simulation and motion base characterization With the physiological
model placed in parallel with the crossover model (see Figure 34), the response of the
pilot model gives insight not only to the overall amplitude ratio response of the

biodynamic system but how each component contributes to the phase of the resulting pilot inputs with respect to the aeroelastic accelerations The overall phase will be demonstrated to have a significant impact on the resulting biodynamic coupling

Figure 42-Figure 46 illustrate the results of the prior simulation with the added impact of modeling biodynamic feedthrough due to aeroelastic accelerations The new simulated pilot performance results are then plotted against the previous rigid body flight simulation

Figure 42 shows the simulated level of involuntary feedthrough along with pilot station (P S) lateral acceleration as the excitation signal, and the resulting lateral stick position This simulated involuntary feedthrough is the resulting stick deflection from the biomechanical feedthrough transfer function, superimposed on the simulated pilot control strategy The resulting sinusoidal motion apparent in the stick signal is predominantly 1 6 Hz, the frequency of the first and dominant resonant mode of the structural model The simulated pilot control strategy still converges on the desired offset, however, until the next, and larger, lateral offset maneuver is commanded at approximately 45 seconds

Figure 43-Figure 45 show the same lateral offset task performed in simulation with biodynamic feedthrough superimposed over the simulated control response In Figure 45, phi and psi represent bank angle and heading angle
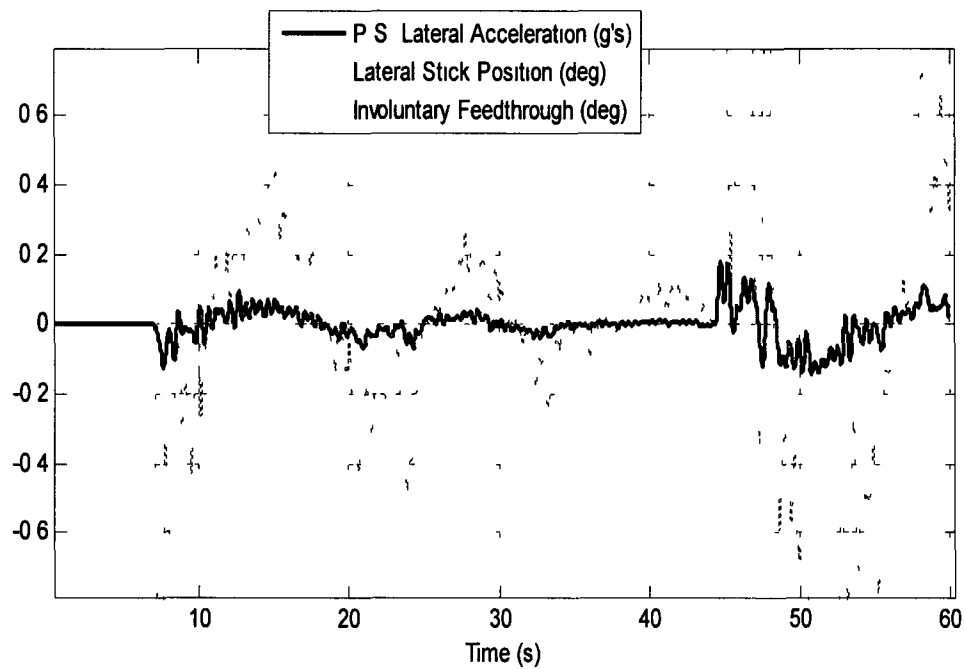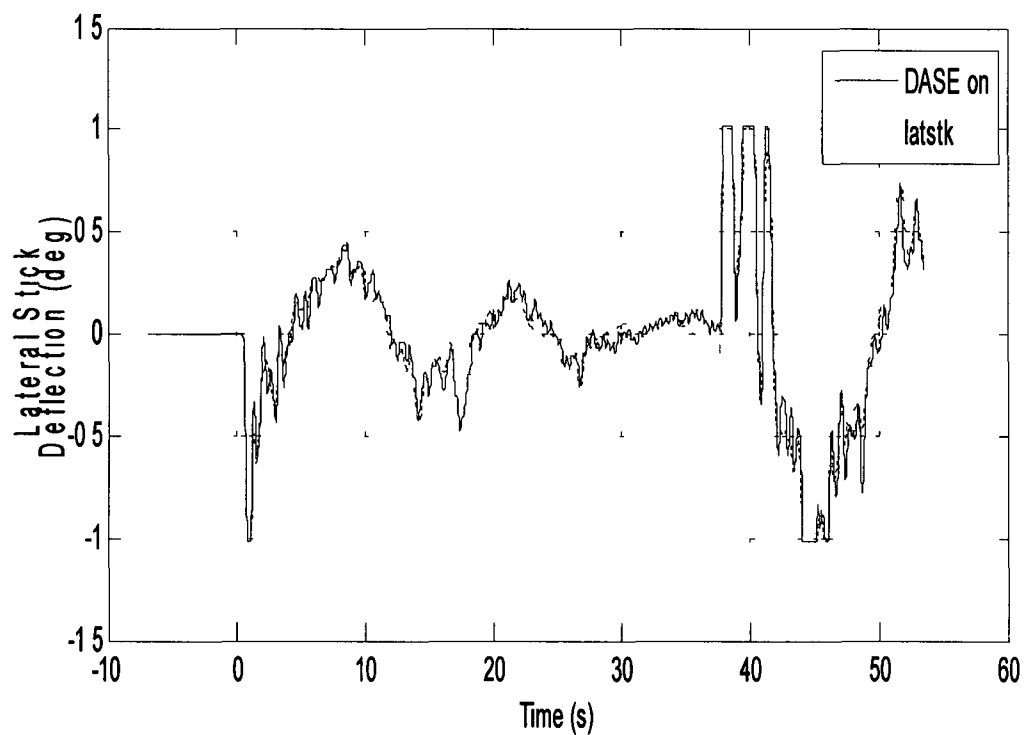
Figure 42 Biodynamic effects

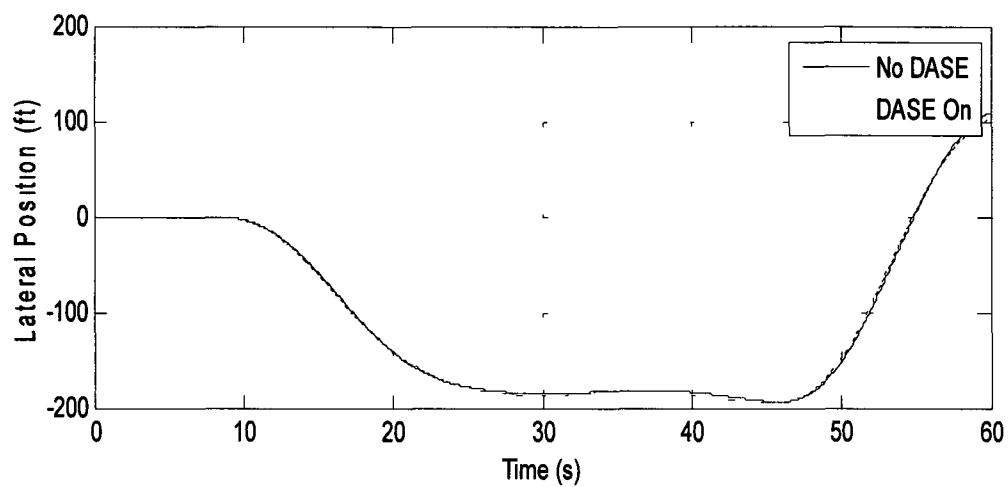**Figure 43 BDC - lateral stick deflection**
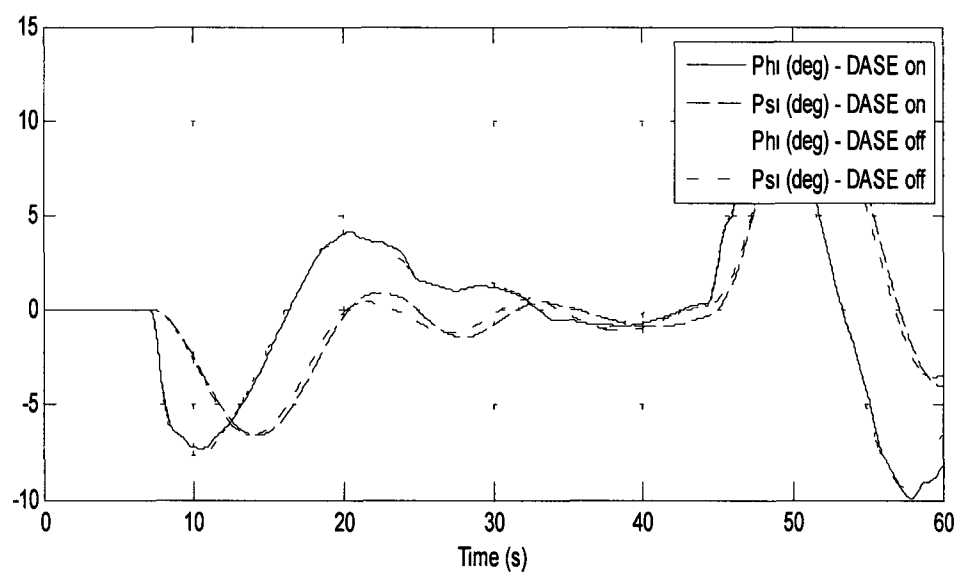
Figure 44 BDC - lateral offset
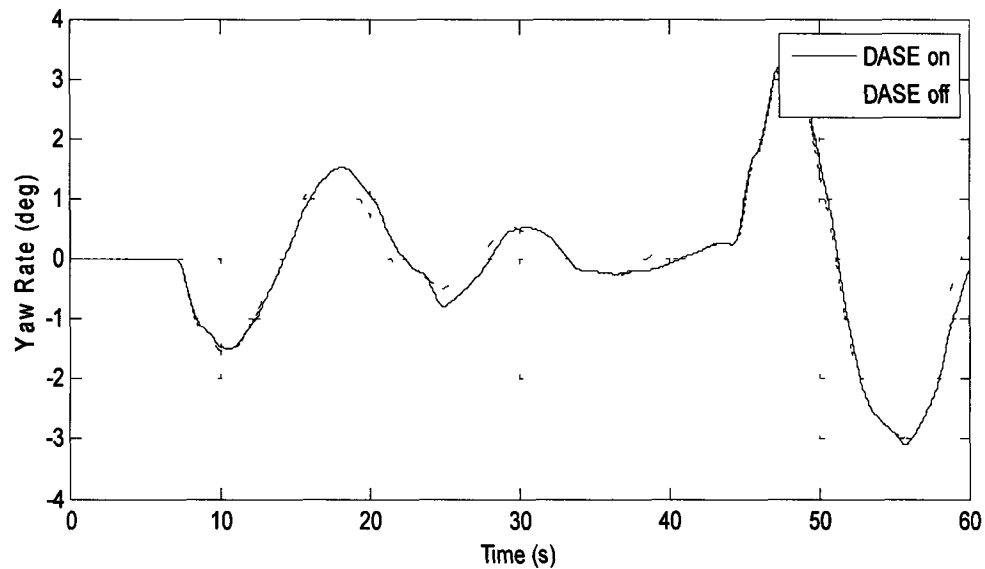

Figure 45 BDC tracked states

Figure 46 DASE on vs DASE off - yaw rate

While the involuntary feedthrough appears to be significant, the simulated pilot still flies the task with similar results This matching could be attributed to the fact that the simulated pilot will receive no degradation in perceived states as the pilot station accelerations grow In actual piloted experiments, pilots noted that as the pilot station accelerations grew, their ability to accurately perceive a large set of current aircraft states diminished A future study to correlate such as degradation in the pilots' processing of their primary inputs as a result of the presence of physical accelerations could be used to create a dynamic visual model This visual model could increase the amount of noise and/or the lag constant simulating the pilots' processing of visual signals

7.2 Simulated Flight

The pilot model can be further used to assess the impact of the lag of the motion base on the experimental results A set of simulated runs were performed for the same lateral offset task with the motion base model removed Thus, the overall phase lag

between commanded accelerations and structural accelerations is decreased These
results are plotted (see Figure 47-Figure 49) against the results from the previous
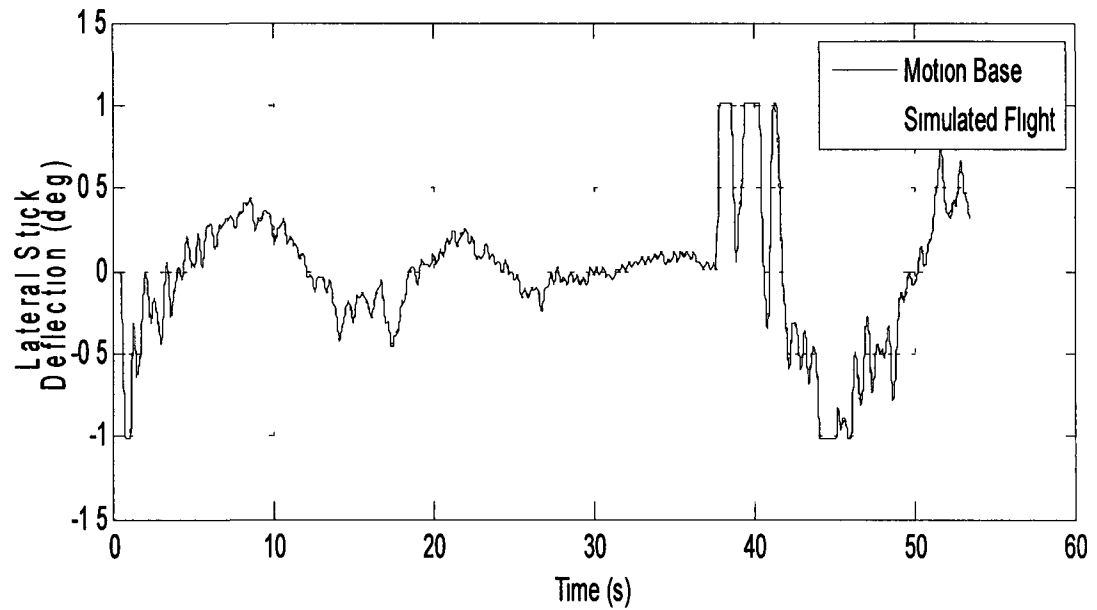simulated lateral offset task with DASE and a simulated motion base

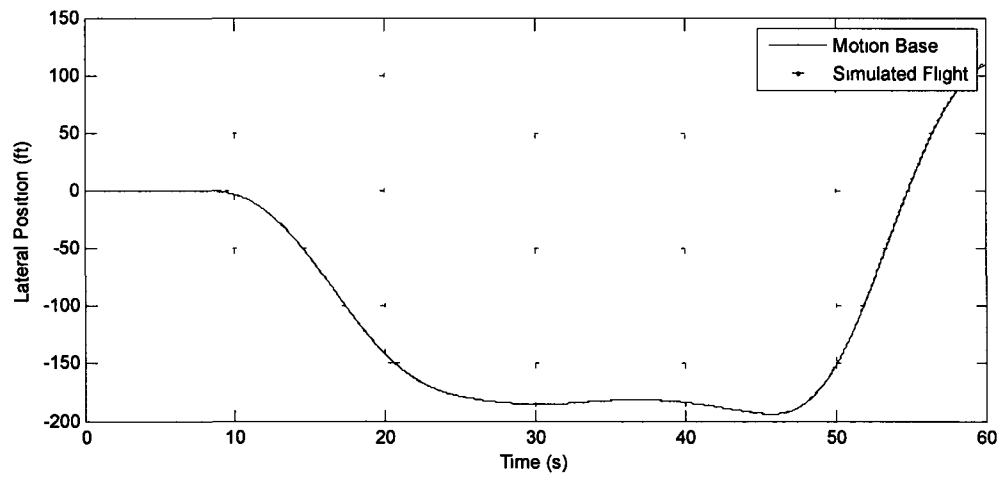Figure 47 Motion base vs simulated flight - lateral stick deflection

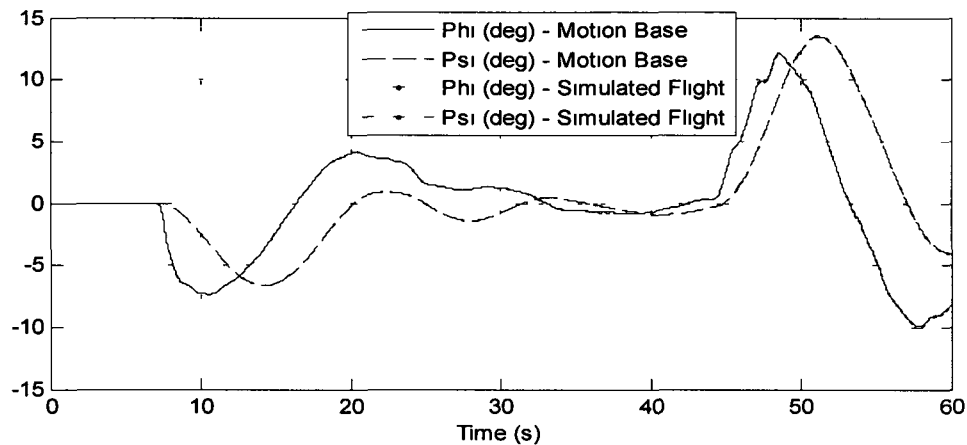Figure 48 Motion base vs simulated flight - lateral position

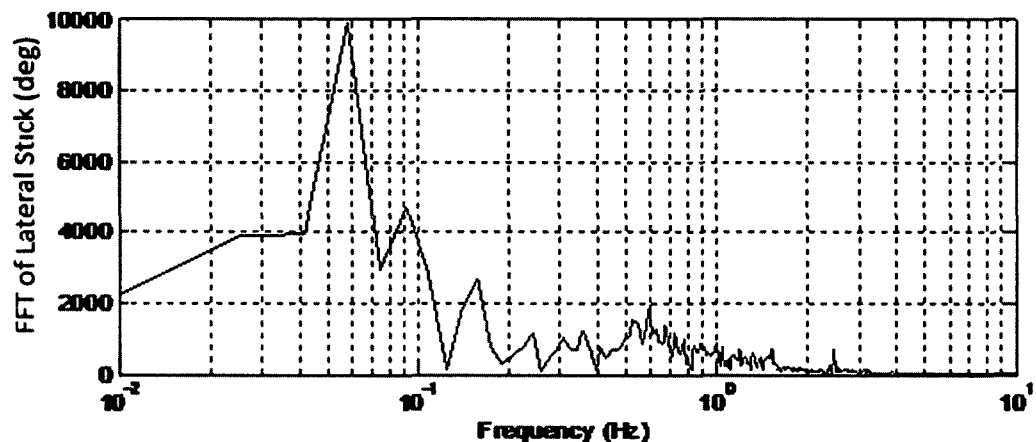**Figure 49 Motion base vs simulated flight - phi and psi**

Figure 50 Motion base vs simulated flight - FFT lateral stick

Figure 47-Figure 50 demonstrate the close match between the simulated flight results and the simulated motion base results This result suggests that the approximate 100 ms phase lag added by the VMS does not significantly impact the levels of biodynamic coupling received The pilot control strategy and the amount of simulated biodynamic feedthrough in both cases match closely However, further simulation shows that such levels of added phase lag can have significant impact on the resulting biodynamic coupling The following section shows the impact of increasing the phase lag of the modeled motion base along with analysis of the resulting biodynamic coupling

7.3 Effects of Phase Lag of VMS

To study the impact of phase lag from the motion base simulator, a pure time delay was added to the motion base model, while the overall amplitude ratio gain of the resulting motion base accelerations are not directly altered As the time delay was increased, the resulting amount of biodynamic coupling decreased up until a delay of 0 1125 s As simulator lag increases above approximately 100 ms, pilot control strategy is typically degraded Thus, the improvement in simulated performance is explained by the decrease in the amount of involuntary feedthrough Figure 51 shows the large attenuation in levels of biodynamic coupling The plots of lateral position and stick frequency response (see Figure 52 and Figure 53) also demonstrate that the task performance is similar to the previous scenarios
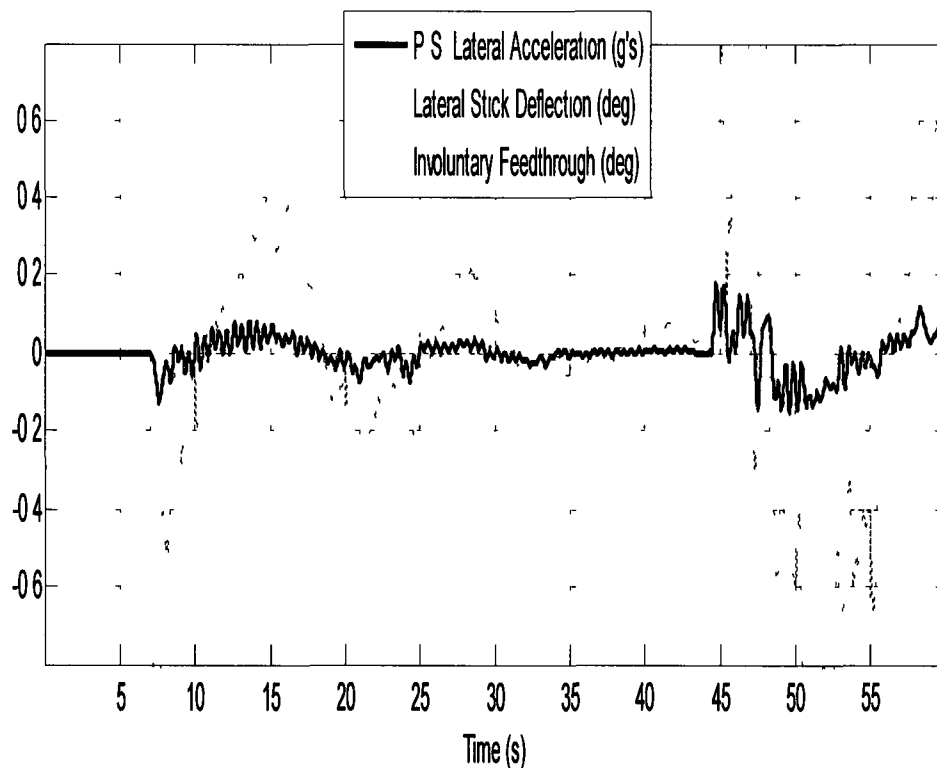

Figure 51 0 1125 sec added time delay – P S lateral acceleration vs lateral stick deflection
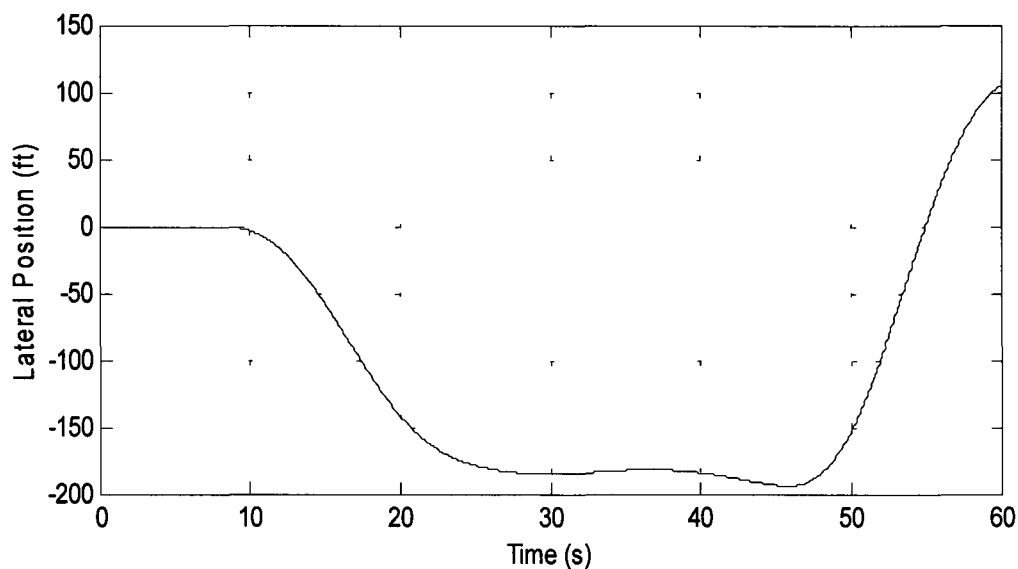
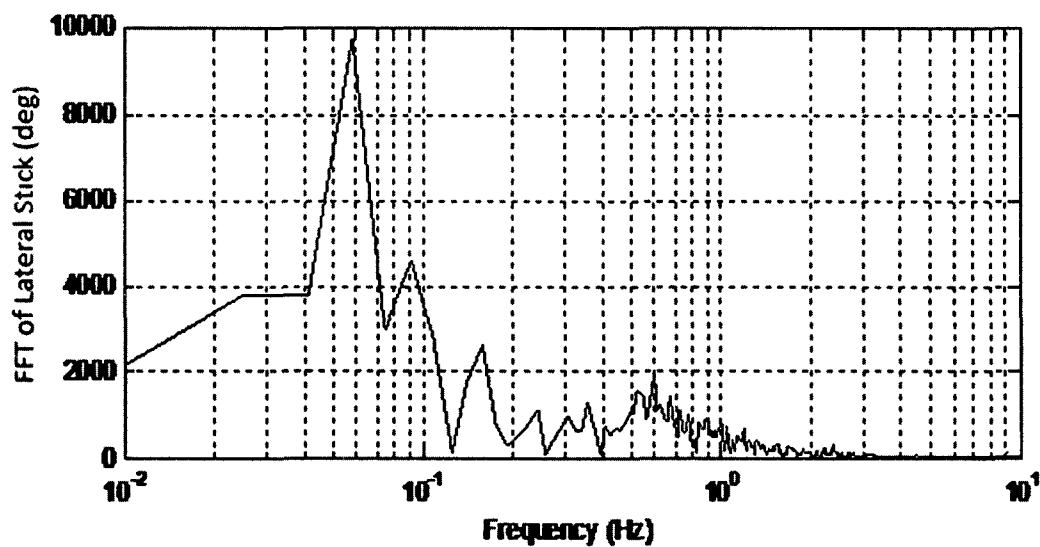Figure 52 0 1125 sec added time delay - lateral position

Figure 53 0 1125 sec time delay - FFT lateral stick

For additional analysis, the added time delay was further increased The resulting biodynamic coupling of the system grew and started to diverge when the added time delay reached 260 ms Figure 54-Figure 56 compared with Figure 51 show the resulting levels of biodynamic coupling and the resulting large pilot station accelerations
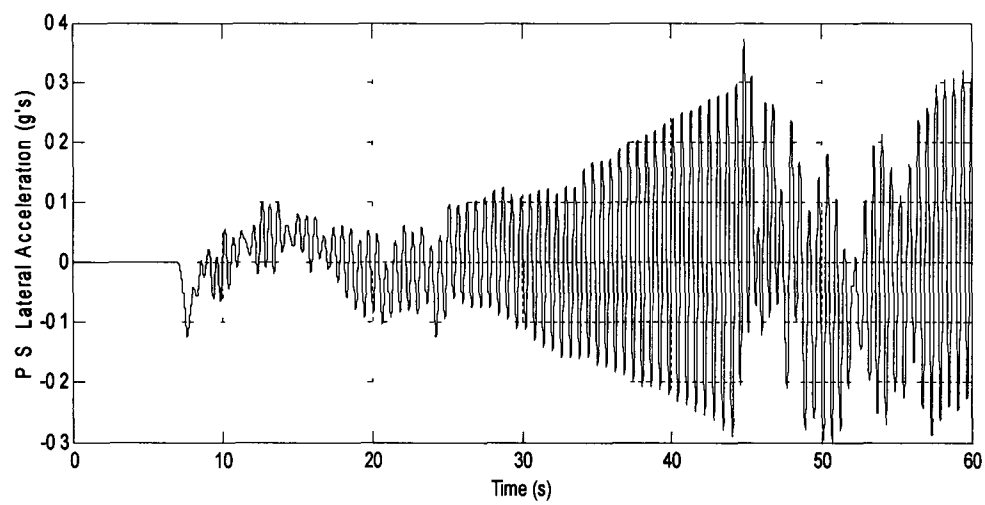
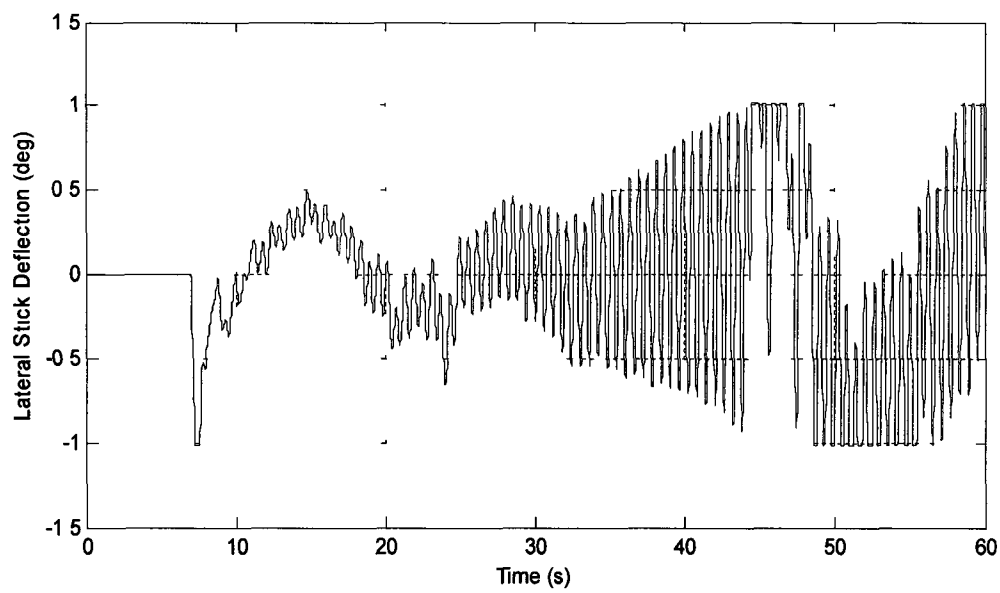**Figure 54 0 2625 sec time delay - lateral acceleration**

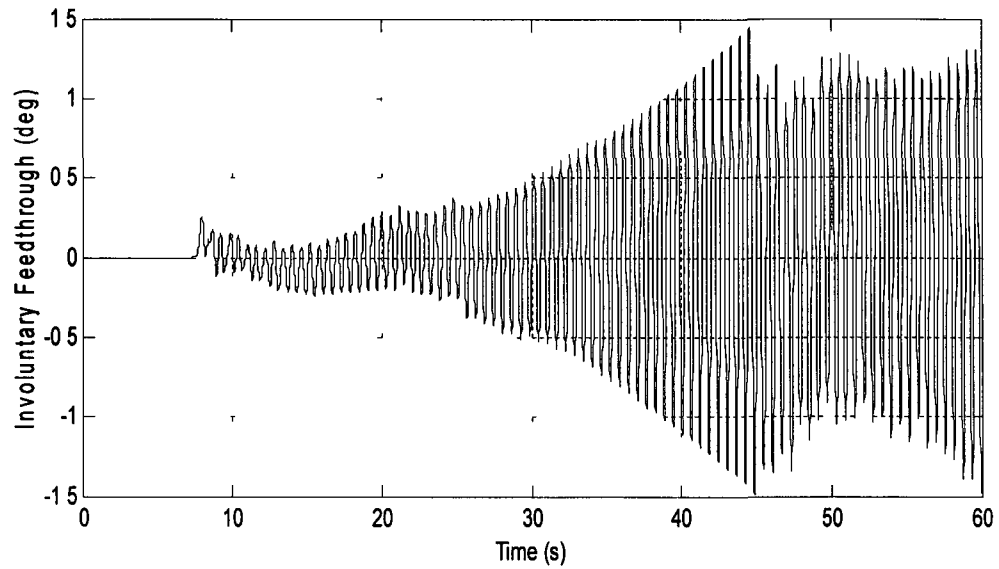**Figure 55 0 2625 sec time delay - lateral stick deflection**

Figure 56 0 2625 sec time delay - involuntary feedthrough

Figure 57 shows the significant peak in energy content of the simulated lateral stick at the same frequency as the first resonant mode
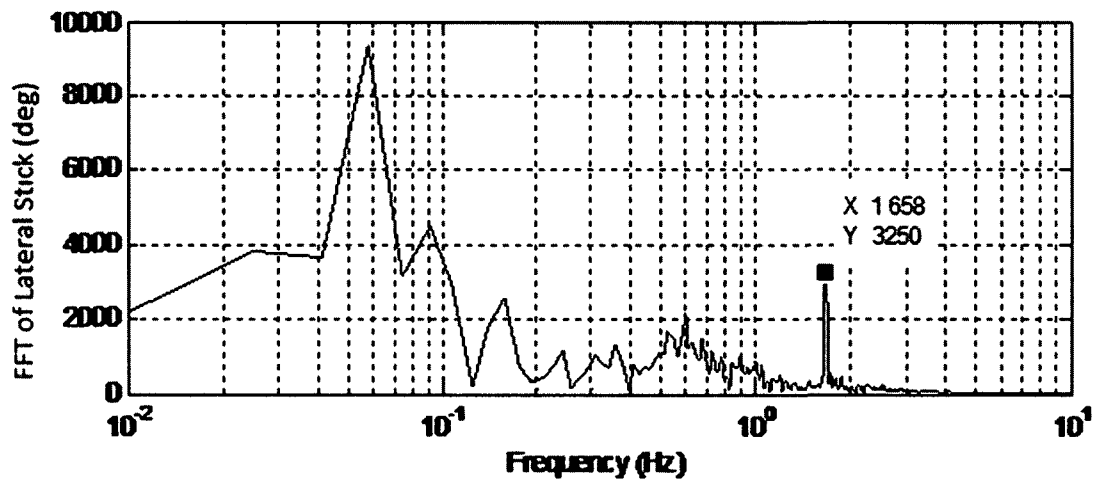

Figure 57 0 2625 sec time delay - FFT of lateral stick

The results clearly show the effects of the pure time delay of the motion base simulator on the overall levels of biodynamic coupling Increasing or decreasing the phase lag can lead to both the attenuation or increase in levels of biodynamic coupling Increasing the pure time delay of the simulated motion base response led to a divergence of motion at the frequency of the structural accelerations shown here

The results show that for the 1 6 Hz first bending mode of this simulated aircraft, the normal phase lag of the motion base does not negatively impact the biodynamic coupling problem However, additional phase lag can degrade performance from biodynamic feedthrough The variance of biodynamic coupling with the phase of the other components of the total system will also exist if sufficiently large The change in levels of biodynamic coupling may depend on the frequency of the dominant resonant mode(s) of the aircraft structure, the frequency of the dominant resonant mode(s) will vary depending on the structure of that particular aircraft

8. CONCLUSION

Biodynamic coupling is a potential problem for supersonic transport aircraft of the future that could tend to have long, slender fuselages To further study this phenomenon, several parametric, piloted studies were performed with supersonic aircraft models These studies found significant possibility of biodynamic coupling during very large maneuvers An additional pilot study was performed to capture the relationship of the involuntary feedthrough of pilot station acceleration through the pilot's body, to the stick A pilot model was constructed from resulting data to simulate the entire pilot-airplane-simulator system

This pilot model predicts both the pilot control strategy and involuntary feedthrough of pilot station acceleration through the stick based From crossover modeling theory, Hess's structural model in multi-loop form was used to predict pilot control strategy The resulting pilot control strategy is based on the lateral offset task performed in the piloted studies

Involuntary feedthrough was modeled in parallel with the structural model assuming no correlation between pilot control strategy and the nature of the involuntary feedthrough Session data were used to construct a LTI system assuming pilot station acceleration as the input and stick deflection as the output

The resulting pilot model was programmed in series with the generic airplane supersonic configuration The generic airplane provided rigid body and dynamics models for manned and batch simulations A model for the motion base simulator was also developed

Modeling the complete pilot-aircraft-motion base system clearly shows the effects of changes in phase of a single component of the system (simulator lag) on the predicted biodynamic coupling of the system Increasing the motion base delay by approximately 100 ms demonstrated a drastic attenuation of the resulting biodynamic coupling, while a further increase of approximately another 100 ms led to diverging structural

accelerations As simulator lag passes approximately 100 ms, pilot control strategy is typically degraded Thus, the improvement in simulated performance is explained by the decrease in the amount of involuntary feedthrough The resulting increase in the biodynamic coupling resulting from further increase in simulator lag implies that the involuntary feedthrough superimposed on the pilot control strategy is passed in phase, increasing the magnitude of the total strategy Furthermore, coupling between the two sources of pilot control causes a divergent closed-loop system

Removing the approximated motion base lag entirely, however, demonstrated little impact on the overall levels of biodynamic coupling This result suggests that previous piloted simulation studies using the VMS with similar dominant resonant modes accurately modeled levels of biodynamic coupling expected in actual flight Piloted runs performed with different structural models, however, may result in experienced levels of biodynamic coupling not representative of actual flight Structural models with prevalent resonant mode frequencies far from 1 6 Hz, particularly of lower frequency, may result in increased amounts of biodynamic coupling as compared to what would be expected from actual flight

Biodynamic coupling is dependent on the entire pilot-airplane-motion simulator system, and thus, the predictions of the impact of the motion base lag will change for different aircraft models, not limited only to a change in the structural dynamics, but also the rigid body dynamics The control interface with the pilot, though not covered in this initial assessment, is also part of this pilot-airplane system This interface would include the stick dynamics and control laws Solutions for preventing biodynamic coupling in a future, supersonic transport design would require analysis for each of these components, with careful analysis of the additional simulator dynamics involved in any preliminary piloted assessment

BIBLIOGRAPHY

1 **McRuer, D and Weir, D H** *Theory of Manual Vehicular Control* 4, 1969, Man-Machine Systems, Vol 10, pp 257-291

2 **Hess, Ronald A.** *Structural Model of the Adaptive Human Pilot* 5, Journal of Guidance and Control, Vol 3 79-1784R

3 **Raney, David L , Jackson, Bruce E. and Buttrill, Carey S** *Simulation Study of Impact of Aeroelastic Characteristics on Flying Qualities of a High Speed Cvil Transport* Washington, D C National Aeronautics and Space Administration, 2002 NASA/TP-2002-211943

4 **Jackson, Bruce E and Raney, David L** *Piloted Simulation Assessment of a High-Speed Civil Transport Configuration* s l National Aeronautics and Space Administration, 2002 NASA/TP-2002-211441

5 **Hoffler, Keith D. and Carzoo, Susan W** *Generic Airplane Model Concept and Four Specific Models Developed for Use in Piloted Simulation Studies* Hampton, VA National Aeronautics and Space Administration, 1997 NASA CR 201651

6 Proceedings of a Workshop of the Dynamic Aeroelastic Modeling Working Group Held August 13-15, 1997 at Langley Research Center Langley Research Center, Hampton, VA National Aeronautics and Space Administration

7 **Telban, Robert J and Cardullo, Frank M.** *Motion Cueing Algorithm Development Human-Centered Linear and Nonlinear Approaches* 2005 NASA/CR-2005-0213747

8 **Parrish, Russel V , Dieudonne, James E and Martin Jr , Dennis J** *Motion Software for a Synergistic Six-Degree-of-Freedom Motion Base* Washington, D C National Aeronautics and Space Administration, 1973 NASA TN D-7350

9 **Gupton, Larry** Operational Readiness Review Cockpit Motion Facility Motion Base Operation of Generic Fligth Deck (GFD) [presentation] Hampton, VA s n , April 9, 2009

10 **Hess, Ronald A** *Feedback Control Models* s l Wiley, 1987, Handbook of Human Factors, p ch 9 5

11 **McRuer, Duane T. and D Graham.** *Analysis of Nonlinear Control Systems* New York Dover, 1971

12 **McRuer, Duane T and Erza S. Krendel** *Mathematical Models of Human Pilot Behavior* s l North Atlantic Treaty Organization Advisory Group for Aerospace Research and Developement , 1974

13 **Hess, Ronald A** *Simplified approach for modelling pilot pursuit control behaviour in multi-loop flight control tasks* 2, 2006, Proceedings of the Institution of Mechanical Engineers, Part G Journal of Aerospace Engineering, Vol 220, pp 85-102

14 **Hess, Ronald A** *Obtaining Mutli-Loop Pursuit-Control Pilot Models From Computer Simulation* s l American Institute of Aeronautics and Astronautics, 2007 AIAA 2007-247

15 **Jex, Henry R and Magdaleno, Raymond E.** *Biomechnical Models for Vibration Feedthrough to Hands and Head For a Semisupine Pilot* 1, 1978, Aviation, Space, and Environmental Medicine, Vol 49, pp 304-316

16 **M., Idan and Merhav, S J** *Effects of Biodynamic Coupling on the Human Operator Model* 4, 1989, Journal of Guidance, Vol 13, pp 630-637

17 **Hess, Ronald A.** *Assessment of Flight Simulator Fidelity in Multiaxis Tasks Including Visual Cue Quality* 6, 1997, Vol 20, pp 11141-1148

18 **Hosman, R. J. A W., and Van Der Vaart, J C** *Vestibular Models and Thresholds of Motion Perception Results of Tests in a Flight Simulator* s l Delft University, April 1978
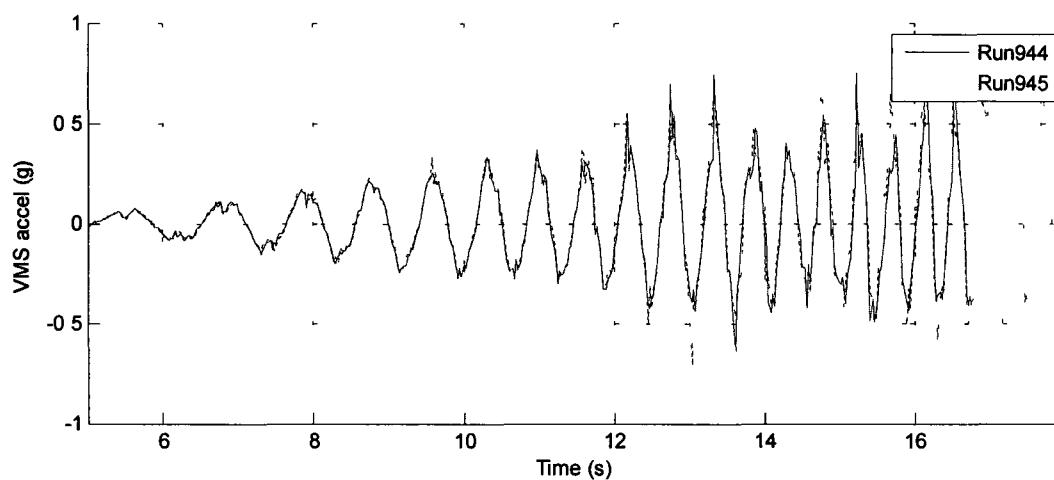
APPENDIX A- Experimental Pilot Study

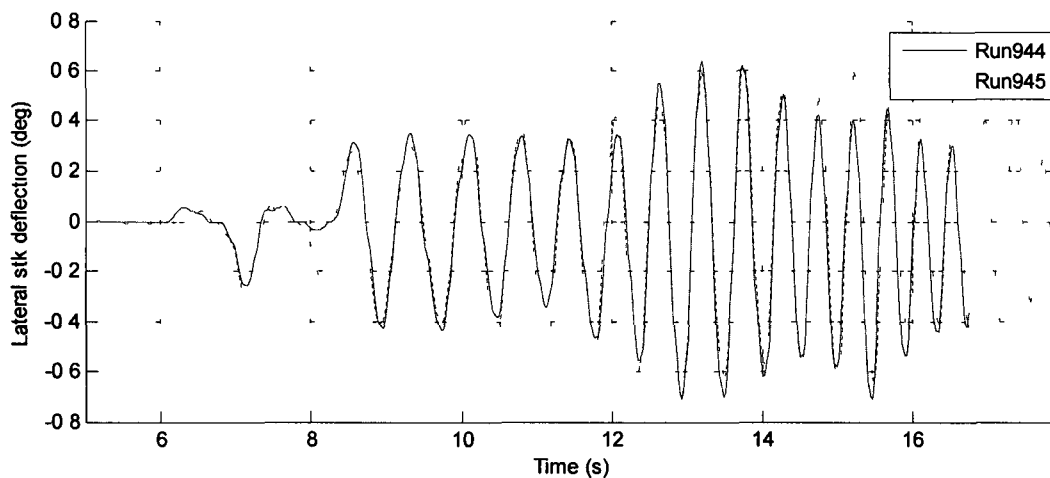**Figure 58 Runs 944 and 945, VMS lateral acceleration**

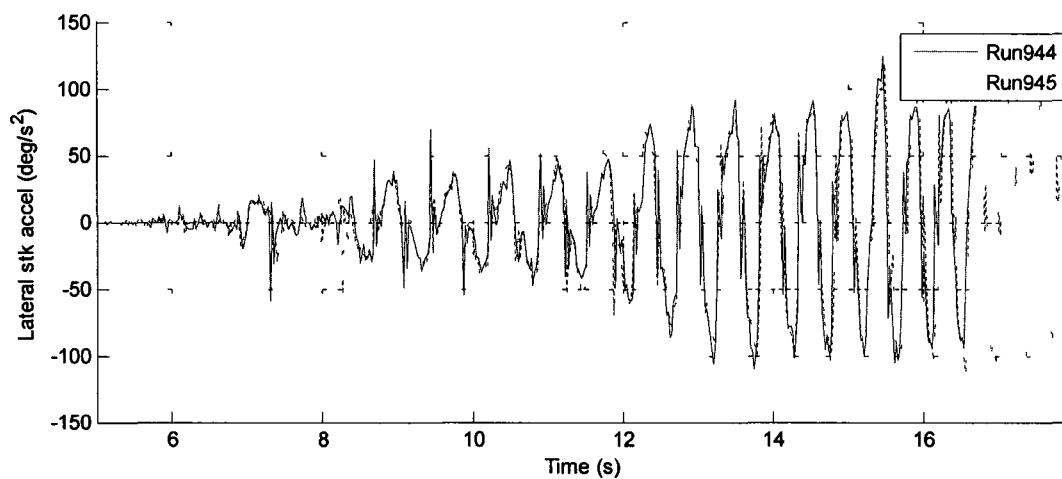**Figure 59 Runs 944 and 945, resulting stick deflection**

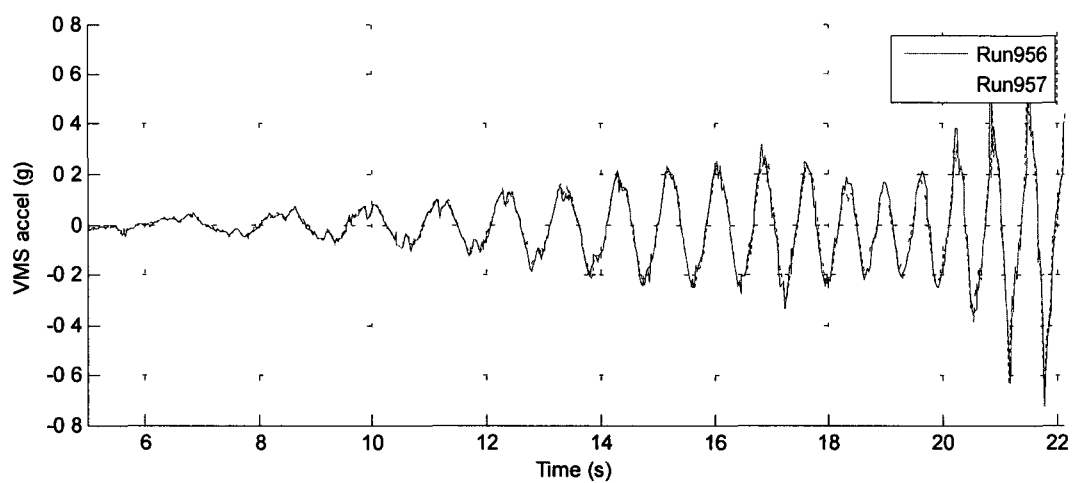**Figure 60 Runs 944 and 945, lateral stick acceleration**

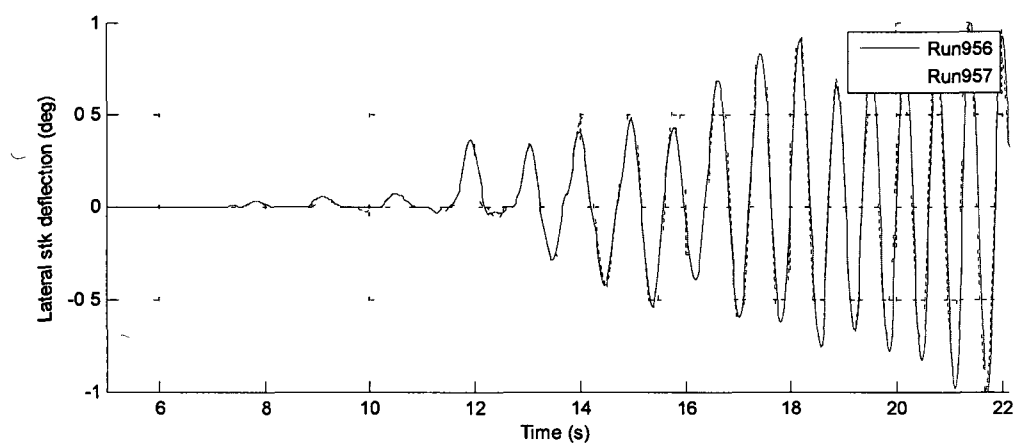**Figure 61 Runs 956 and 957, VMS lateral acceleration**

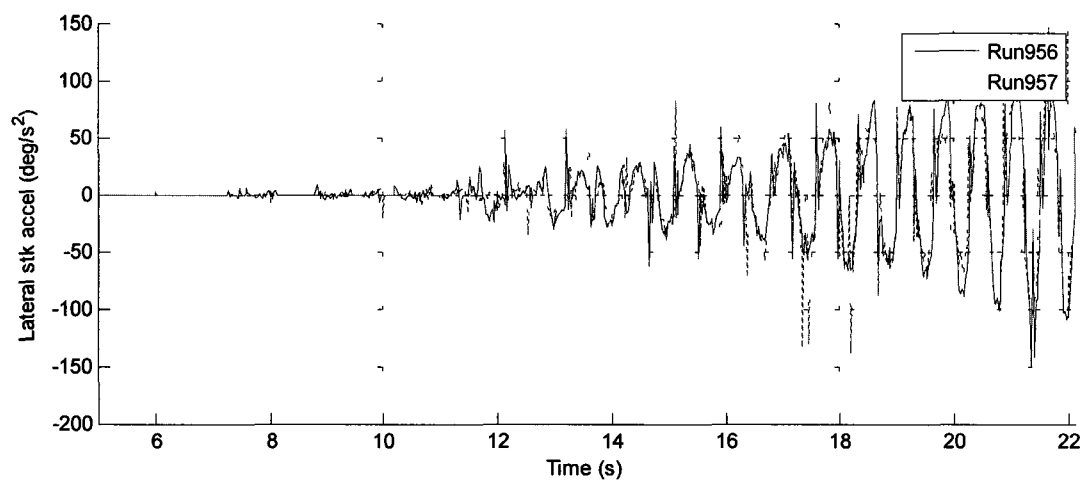**Figure 62 Runs 956 and 957, resulting stick deflection**

Figure 63 Runs 956 and 957, resulting stick acceleration

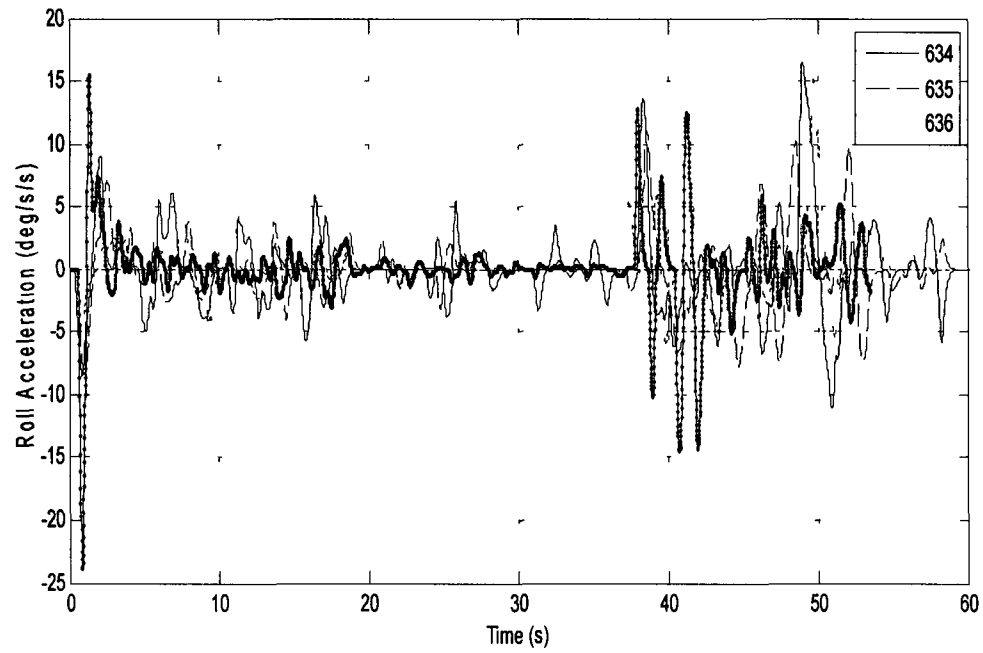# APPENDIX B – Simulated Pilot Control Strategy

Figure 64 Crossover model vs empirical pilot - roll rate

VITA

Brandon Cowen is currently working for Adaptive Aerospace Group He graduated from Embry-Riddle Aeronautical University in 2007 with a Bachelor of Science in Aerospace Engineering He attended Old Dominion University from 2008 to 2011 for a Master of Science in Aerospace Engineering